

Article

A Hidden Side of the Conformational Mobility of the Quercetin Molecule Caused by the Rotations of the O3H, O5H and O7H Hydroxyl Groups: *In Silico* Scrupulous Study

Ol'ha O. Brovarets^{1,*}  and Dmytro M. Hovorun^{1,2}

- ¹ Department of Molecular and Quantum Biophysics, Institute of Molecular Biology and Genetics, National Academy of Sciences of Ukraine, 150 Akademika Zabolotnoho Street, 03680 Kyiv, Ukraine; d.m.hovorun@imbg.org.ua
- ² Department of Molecular Biotechnology and Bioinformatics, Institute of High Technologies, Taras Shevchenko National University of Kyiv, 2-h Akademika Hlushkova Avenue, 03022 Kyiv, Ukraine
- * Correspondence: o.o.brovarets@imbg.org.ua

Received: 6 December 2019; Accepted: 16 January 2020; Published: 3 February 2020



Abstract: In this study at the MP2/6-311++G(2df,pd)//B3LYP/6-311++G(d,p) level of quantum-mechanical theory it was explored conformational variety of the isolated quercetin molecule due to the mirror-symmetrical hindered turnings of the O3H, O5H and O7H hydroxyl groups, belonging to the A and C rings, around the exocyclic C–O bonds. These dipole active conformational transformations proceed through the 72 transition states (TSs; C_1 point symmetry) with non-orthogonal orientation of the hydroxyl groups relatively the plane of the A or C rings of the molecule ($\text{HO}_7\text{C}_7\text{C}_8/\text{HO}_7\text{C}_7\text{C}_6 = \pm(89.9\text{--}93.3)$, $\text{HO}_5\text{C}_5\text{C}_10 = \pm(108.9\text{--}114.4)$ and $\text{HO}_3\text{C}_3\text{C}_4 = \pm(113.6\text{--}118.8$ degrees) (here and below signs ‘±’ corresponds to the enantiomers)) with Gibbs free energy barrier of activation $\Delta\Delta G_{\text{TS}}$ in the range 3.51–16.17 kcal·mol⁻¹ under the standard conditions ($T = 298.1$ K and pressure 1 atm): $\Delta\Delta G_{\text{TS}}^{\text{O}_7\text{H}} (3.51\text{--}4.27) < \Delta\Delta G_{\text{TS}}^{\text{O}_3\text{H}} (9.04\text{--}11.26) < \Delta\Delta G_{\text{TS}}^{\text{O}_5\text{H}} (12.34\text{--}16.17 \text{ kcal mol}^{-1})$. Conformational dynamics of the O3H and O5H groups is partially controlled by the intramolecular specific interactions O3H … O4, C2'/C6'H … O3, O3H … C2'/C6', O5H … O4 and O4 … O5, which are flexible and cooperative. Dipole-active interconversions of the enantiomers of the non-planar conformers of the quercetin molecule (C_1 point symmetry) is realized via the 24 TSs with C_1 point symmetry ($\text{HO}_3\text{C}_3\text{C}_2\text{C}_1 = \pm(11.0\text{--}19.1)$, $\text{HC}_2'\text{/C}_6'\text{C}_1'\text{C}_2 = \pm(0.6\text{--}2.9)$ and $\text{C}_3\text{C}_2\text{C}_1'\text{C}_2'\text{/C}_3\text{C}_2\text{C}_1'\text{C}_6' = \pm(1.7\text{--}9.1)$ degree; $\Delta\Delta G_{\text{TS}} = 1.65\text{--}5.59 \text{ kcal mol}^{-1}$), which are stabilized by the participation of the intramolecular C2'/C6'H … O1 and O3H … HC2'/C6' H-bonds. Investigated conformational rearrangements are rather quick processes, since the time, which is necessary to acquire thermal equilibrium does not exceed 6.5 ns.

Keywords: quercetin molecule; conformational mobility; transition state; hydroxyl group; enantiomer; mirror symmetry; point symmetry; unusual H-bond; quantum-mechanical calculation; AIM analysis

1. Introduction

Quercetin molecule is one of the important flavonoids and has a broad range of anti-oxidant, anti-inflammation and others therapeutic actions [1–7]. This compound, which consists of (A + C) and B rings and five OH hydroxyl groups at the 3, 3', 4', 5 and 7 positions [8–13], is usually gained from plants, vegetables and fruits like blueberries, apples, green tea, wine and onion. At the same time, it possesses low solubility in water and poor permeability in physiological solutions, which limits its application in the pharmaceutical field [14]. It was the object of the theoretical analysis, in particular with the application of the quantum-chemical methods [11,15].

In our previous study it was found by using the quantum-mechanical (QM) calculations at the MP2/6-311++G(2df,pd)//B3LYP/6-311++G(d,p) level of QM theory that isolated quercetin molecule is very conformationally mobile structure and so can acquire 48 stable conformers, among which there are 24 planar (C_s point symmetry) and 24 non-planar (C_1 point symmetry) with Gibbs free energy ranging from 0.00 to 25.30 kcal·mol⁻¹ under standard conditions and with a dipole moment, which varies from 0.35 to 9.87 Debye [16]), which can interconvert into each other through the rotations of its non-deformable (A + C) and B rings around the C2–C1' bond [17–20].

At this, all possible conformers can be divided into four different subfamilies, depending on the orientations of the (A + C) and B rings and 5 hydroxyl groups of the quercetin molecule: subfamily I—conformers 1–12; subfamily II—conformers 13–18, 20, 23, 24, 26, 29 and 30; subfamily III—conformers 19, 21, 22, 25, 27, 28, 31–36 and subfamily IV—conformers 37–48 (see Figure 2 in the paper [16]). Planar conformers belong to the subfamilies I and III, non-planar ones—to the subfamilies II and IV.

However, despite the intensive theoretical investigations of the conformational properties of the quercetin molecule [1–27], information according the fundamental mechanisms of the conformational transitions, which are caused by the torsional mobility of its hydroxyl groups around the exocyclic C–O bonds, remains very restricted.

In this study we pursued the goal to investigate the conformational mobility of the quercetin molecule, which is defined by the rotations of the O3H, O5H and O7H hydroxyl groups around the exocyclic C3–O3, C5–O5 and C7–O7 bonds through the transitions states, and also to establish the pathways of the interconversion of the enantiomers of all its non-planar conformers.

Importance of such set of the task is caused by the torsional mobility of the O3H and O5H hydroxyl groups, which is mostly responsible for the formation of the three conformational subfamilies, while the torsional mobility of the O7H hydroxyl group plays the role at this of the additional “multiplier” of the conformational states. The multifunctionality of the quercetin molecule of natural origin is usually associated with its conformational diversity [2,7,8,10].

Many of the biological molecules (and quercetin in this case is not the exception) commonly have various enantiomers, which differently effect on living systems. Notably, that opposite to the objects of the non-living nature, the “R” and “L” forms in them have different part of the observance. Thus, in particular, native proteins contain only “L” amino acids, while nucleic acids—only “R” sugar residues.

It is also known that among drugs very often only one of the enantiomers is responsible for the desired physiological effects, while another enantiomer is less important or even leads to genuinely opposite effect. That is why very often the drug is based only on one enantiomer in order to increase its activity and eliminate ‘side effects’. So, it is important to know the possible ways of the interconversion of the enantiomers of the biomolecules between each other [28,29].

As a result of this in-depth *in silico* investigation at the MP2/6-311++G(2df,pd)//B3LYP/6-311++G(d,p) level of QM theory, we defined all possible conformational pathways of the rotations of the O3H, O5H and O7H hydroxyl groups, and also their physico-chemical characteristics such as geometrical, in particular symmetrical, energetic and polar, which are reflecting the details of the biological mechanisms of action of the quercetin molecule. Intramolecular specific contacts, H-bonds and attractive van der Waals (vdW) contacts, which assist these biologically-important processes and represent biologically important structural attribute of the quercetin molecule [16,17], have also been explored in detail.

2. Computational Methods

Calculations of the geometries of the conformers and transition states (TSs) of their interconversions, followed by the calculations of their vibrational spectra scaled by a factor of 0.9668 [30], have been performed at the B3LYP/6-311++G(d,p) level of QM theory [31–33] by Gaussian'09 program package [34]. This quantum-chemical level of theory has been approved to show adequate results at the studies of heterocyclic compounds [35,36].

Intrinsic reaction coordinate (IRC) calculations has been performed using Hessian-based predictor-corrector integration algorithm [37] by following in the forward and reverse directions from each TS, containing one and only one imaginary frequency in the vibrational spectra.

All calculations have been provided for the quercetin molecule as its intrinsically inherent property.

Electronic and Gibbs free energies under standard conditions have been calculated at the MP2/6-311++G(2df,pd)//B3LYP/6-311++G(d,p) level of QM theory [38–40].

The time $\tau_{99.9\%}$, which is needed for reaching the 99.9% of the equilibrium concentration of the reactant and product has been calculated by the formula [41]:

$$\tau_{99.9\%} = \frac{\ln 10^3}{k_f + k_r}, \quad (1)$$

where forward k_f and reverse k_r rate constants for the conformational transitions have been obtained by the formula [41]:

$$k_{f,r} = \Gamma \cdot \frac{k_B T}{h} e^{-\frac{\Delta \Delta G_{f,r}}{RT}}, \quad (2)$$

where Γ —Wigner’s coefficient, accounting tunneling [42]:

$$\Gamma = 1 + \frac{1}{24} \left(\frac{h v_i}{k_B T} \right)^2, \quad (3)$$

where k_B —Boltzmann’s constant, h —Planck’s constant, $\Delta \Delta G_{f,r}$ —Gibbs free energy of activation for the conformational transition in the forward (f) and reverse (r) directions and v_i —magnitude of the imaginary frequency of the vibrational mode at the TSs.

The lifetime τ of the conformers has been obtained using the formula:

$$\tau = 1/k_r. \quad (4)$$

The topology of the electron density was analyzed by AIM’2000 program package [43,44], based on the Bader’s quantum theory of “Atoms in Molecules” (QTAIM). For this purpose it was used wave functions received at the B3LYP/6-311++G(d,p) level of QM theory.

Energies of the unusual intramolecular CH···OH-bonds and OH...HC dihydrogen bonds [45] and attractive O···O vdW contacts [16,17] have been calculated by the empirical Espinosa–Molins–Lecomte (EML) formula [46,47]:

$$E_{\text{CH}\cdots\text{O}/\text{OH}\cdots\text{HC}/\text{O}\cdots\text{O}} = 0.5 \cdot V(r), \quad (5)$$

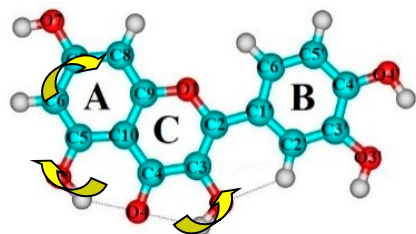
where $V(r)$ —value of a local potential energy at the (3, -1) BCP.

The energies of the classical intramolecular OH···OH-bonds have been received by the Nikolaienko–Bulavin–Hovorun (NBH) formula [48]:

$$E_{\text{OH}\cdots\text{O}} = -3.09 + 239 \cdot \rho, \quad (6)$$

where ρ —the electron density at the (3, -1) BCP of the H-bond.

In this work standard numeration of the atoms of the quercetin molecule was used [16,17] (see Scheme 1).



Scheme 1. Representation of the structure of the quercetin molecule and numbering of its atoms. Rotations of the O₃H, O₄H and O₅H hydroxyl groups are designated by the yellow arrows.

3. Results and Discussion

Aiming to achieve the goal set in this work and obtain maximally possible information according to the conformational properties of the quercetin molecule, which is connected with the mirror-symmetric turnings of the hydroxyl groups in the 3, 5 and 7 positions around the corresponding exocyclic C–O bonds, we localized all possible 72 TSs (24 for each hydroxyl group—O₃H, O₅H and O₇H), which were controlling these processes (see for more details Figures 1–4 and Tables 1–5). This enabled us to receive a complete picture of the conformational mobility and to obtain a number of interesting physico-chemical regularities.

Thus, all established TSs (C_1 point symmetry; Figures 1–3, Tables 1–3 and Table 5) have non-orthogonal structure—corresponding dihedral angles, which describe the orientation of the OH hydroxyl groups according to the rings, to which they are covalently bonded, lie in the range $\pm(89.9\text{--}93.3)/\pm(108.9\text{--}114.4)/\pm(113.6\text{--}118.8)$ degrees (signs “ \pm ” correspond to enantiomers). This fact is connected with the asymmetrical surrounding of the lone electron pairs of the oxygen atom of the hydroxyl groups. In the process of the turning via the TSs it was not observed deformation of the hydroxyl groups or rings, with which they are bounded. In other words, these fragments of the quercetin molecule could be considered as non-deformational, rigid rotators. Turning of the O₅H and O₇H around the 180 degree around the C₅–O₅ and C₇–O₇ bonds practically do not change the geometry of the molecule. At the same time, the torsional mobility of the O₃H hydroxyl group is closely connected with the torsional mobility of the B ring around the C₂–C_{1'} bond (Figures 1–3, Tables 1–3 and Table 5).

Interestingly, that TSs, which control the torsional mobility of the O₃H and O₅H hydroxyl groups, are stabilized by the intramolecular specific interactions (Figure 2, Figure 3 and Table 5). The same effects are not characteristic for the rotation of the O₇H hydroxyl group (Figure 1).

In the first case for the O₃H hydroxyl group turning—there are non-standard [45] C_{2'}H/C_{6'}H...O₃H H-bonds ($2.86\text{--}2.99/2.83\text{--}2.95 \text{ kcal}\cdot\text{mol}^{-1}$); in the second case—attractive O₄...O₅ vdW contact ($2.91\text{--}3.27 \text{ kcal}\cdot\text{mol}^{-1}$). It should be noted that energies of these interactions in TSs are higher, than in the corresponding conformers—starting in the first case and terminal—in the second case [16].

It attracts attention that at the TSs^{O₇H}, where O₇H hydroxyl group is not involved in the intramolecular specific interactions, the energy of all others specific interactions (O₅H ... O₄, O₃H ... O₄, O₃H ... C_{2'}/C_{6'}, C_{2'}/C_{6'}H ... O₃ and O₄ ... O₅), especially of two first, slightly changes (no more than by 5%) in comparison with the analogous values for the starting or terminal conformers. It points on the fact, that strictly saying, specific intramolecular contacts are not interactions, which are localized at the defined set of atoms and are dependent on the conformational state of the whole molecule.

It was observed interesting dependencies of the influence of the rotation of the hydroxyl group around the C–O bond on the energy of the specific intramolecular interactions for the TSs^{O₅H} (Figure 2, Tables 2 and 5). In the case of the conformational transitions in the non-planar conformers of the quercetin molecule this influence on the energies of the O₃H ... C_{2'}/C_{6'} H-bonds and attractive O₄ ... O₅ vdW contacts could be neglected, since it is insignificant. Transition of the O₅H hydroxyl group at the TSs of the planar conformers caused insignificant increasing of the energy (by $0.07 \text{ kcal mol}^{-1}$) of the O₄ ... O₅ contact in comparison with the final conformers. At the same time, the energy of the O₃H ... O₄ H-bond significantly increased (by 40%) in comparison with the analogous values for the

starting conformers, and the energy of the C2'/C6'H ... O3 H-bonds remained almost unchangeable (Table 5).

At the transition of the O3H group at the TSs, the energy of the C2'/C6'H ... O3 H-bonds decreased by 25%, and energy of the O5H ... O4 H-bonds increased by 30% in comparison with the analogous value for the starting conformers. At the same time, the energy of the attractive O4 ... O5 vdW contacts increased by 0.3% in comparison with the analogous value for the starting conformers (Table 5).

Under standard conditions the activation barriers of the Gibbs free energies $\Delta\Delta G_{TS}$ form the following order of priority: $\Delta\Delta G_{TS}^{O7H}$ (3.51–4.24) < $\Delta\Delta G_{TS}^{O3H}$ (9.04–11.26) < $\Delta\Delta G_{TS}^{O5H}$ (12.34–16.17 kcal mol⁻¹; Tables 1–3). It became understandable from the mentioned above, why the value of the Gibbs free energy barrier for the forward conformational transformation $\Delta\Delta G_{TS}^{O5H}$ is the largest—at the corresponding TSs the most strong O5H ... O4 H-bonds (6.47–8.62 kcal·mol⁻¹) was absent and could not be compensated by the present attractive O4 ... O5 vdW contact (2.97–3.27 kcal·mol⁻¹) and increasing of the energy of the unusual [45] C2'H/C6'H...O3 H-bond on 1.3 kcal mol⁻¹ (Table 5). Value of the $\Delta\Delta G_{TS}^{O7H}$ was the smallest, since in this case there were no specific intramolecular interactions. Value for the $\Delta\Delta G_{TS}^{O3H}$ possessed a middle value, since the absence of the O3H ... O4 H-bond (3.12–4.56 kcal·mol⁻¹) was partially compensated by the non-standard [45] C2'H/C6'H...O3 H-bonds (2.85–2.95 kcal·mol⁻¹; Table 5).

By analyzing the rearrangement of the specific intramolecular contacts (H-bonds and vdW contacts) it was established that in the case of the rotation of the O7H hydroxyl group these contacts remained (Figures 1–3, Table 5). In particular, in the case of the interconversion of the planar conformers of the quercetin molecule there were three specific contacts:

- O5H ... O4, O3H ... O4 and C2'H ... O3 H-bonds (initial conformer, TS, terminal conformer; 1↔5, 7↔8 and 10↔12);
- O5H ... O4, O3H ... O4 and C6'H ... O3 H-bonds (initial conformer, TS, terminal conformer; 2↔4, 3↔6 and 9↔11);
- O5 ... O4 vdW contact and O3H ... O4, C2'H ... O3 H-bonds (initial conformer, TS, terminal conformer; 19↔25, 27↔32 and 33↔35);
- O5 ... O4 vdW contact and O3H ... O4, C6'H ... O3 H-bonds (initial conformer, TS, terminal conformer; 21↔31, 22↔28 and 34↔36).

In the case of the interconversion of the non-planar conformers there were two specific contacts:

- O5H ... O4 and O3H ... C6' H-bonds (initial conformer, TS, terminal conformer; 13↔23, 14↔17 and 24↔29);
- O5H ... O4 and O3H ... C2' H-bonds (initial conformer, TS, terminal conformer; 15↔18, 16↔20 and 26↔30);
- O5 ... O4 vdW contact and O3H ... C6' H-bond (initial conformer, TS, terminal conformer; 37↔43, 39↔44 and 45↔47);
- O5 ... O4 vdW contact and O3H ... C2' H-bond (initial conformer, TS, terminal conformer; 38↔41, 40↔42 and 46↔48).

Notably, that for each set of the specific intramolecular contacts, there were three transitions.

In the case of the rotation of the O5H hydroxyl group the set of intramolecular specific contacts (3 H-bonds) transformed into the set of 1 vdW contact and 2 H-bonds for the interconversions of the planar conformers:

- O5H ... O4, O3H ... O4 and C2'H ... O3 H-bonds (initial conformer) → O5 ... O4 vdW contact and O3H ... O4, C2'H ... O3 H-bonds (TS, terminal conformer; 1↔25, 3↔28, 5↔19, 7↔32, 8↔27, 10↔35 and 12↔33);
- O5H ... O4, O3H ... O4 and C6'H ... O3 H-bonds (initial conformer) → O5 ... O4 vdW contact and O3H ... O4, C6'H ... O3 H-bonds (TS, terminal conformer; 2↔31, 4↔21, 6↔22, 9↔36 and 11↔34).

A set of two intramolecular contacts (2 H-bonds) transformed into another set (1 vdW contact and 1 H-bond) for the interconversions of the non-planar conformers:

- O5H ... O4 and O3H ... C6' H-bonds (initial conformer) → O5 ... O4 vdW contact and O3H ... C6' H-bonds (TS, terminal conformer; **13↔43, 14↔44, 17↔39, 23↔37, 24↔47** and **29↔45**);
- O5H ... O4 and O3H ... C2' H-bonds (initial conformer) → O5 ... O4 vdW contact and C6'H ... O3 H-bonds (TS, terminal conformer; **15↔42, 16↔38, 18↔40, 20↔41, 26↔48** and **30↔46**).

Finally, the most exotic situation was observed at the interconversion of the conformers, which all were non-planar, through the rotation of the O3H hydroxyl group—at this, three intramolecular specific contacts (3 H-bonds/1 vdW contact and 2 H-bonds) transformed into two (2 H-bonds/1 vdW contact and 1 H-bond):

- O5H ... O4, O3H ... O4 and C2'H ... O3 H-bonds (initial conformer) → O5H ... O4, C2'H ... O3H H-bonds (TS) → O5H ... O4 and O3H ... C2' H-bonds (terminal conformer; **1↔20, 5↔16, 7↔15, 8↔18, 10↔26** and **12↔30**);
- O5H ... O4, O3H ... O4 and C6'H ... O3 H-bonds (initial conformer) → O5H ... O4, C6'H ... O3H H-bonds (TS) → O5H ... O4 and O3H ... C6' H-bonds (terminal conformer; **2↔14, 3↔13, 4↔17, 6↔23, 9↔24** and **11↔29**);
- O5 ... O4 vdW contact and O3H ... O4, C2'H ... O3 H-bonds (initial conformer) → O5 ... O4 vdW contact and C2'H ... O3H H-bond (TS) → O5 ... O4 vdW contact and O3H ... C2' H-bond (terminal conformer; **19↔38, 25↔41, 27↔40, 32↔42, 33↔46** and **35↔48**);
- O5 ... O4 vdW contact and O3H ... O4 and C6'H ... O3 H-bonds (initial conformer) → O5 ... O4 vdW contact and C6'H ... O3H H-bond (TS) → O5H ... O4 and O3H ... C6' H-bonds (terminal conformer; **21↔39, 22↔37, 28↔43, 31↔44, 34↔45** and **36↔47**).

It attracted attention that behavior of the O7H hydroxyl group significantly differed from the other two hydroxyl groups—at its turning on 180 degrees around the C7–O7 bond relative Gibbs free energy of the molecule changed insignificantly (no more than on $0.75 \text{ kcal}\cdot\text{mol}^{-1}$) with four exceptions (Table 1). Moreover, dihedral angle HO7C7C8/HO7C7C6, which describes the orientation of this group in the transition state relatively the A ring, differs from the right angle maximally by the 3.4 degree (Table 1).

Since the hydroxyl group was quite polar fragment, it is understandable, that all 72 conformational transitions without exceptions were dipole-active (Figures 1–3, Tables 1–3). That is, they were accompanied by the significant changing of the dipole moment of the molecule as by the absolute value, so by the spatial orientation.

Revealed conformational processes were in the range from $5.6\cdot10^{-15}$ to $1.7\cdot10^{-10} \text{ s}$ —time, which is necessary to acquire thermal equilibrium, did not exceed 6.5 ns (Tables 1–3).

The calculations revealed four dynamically unstable conformers—**20, 23, 43** and **44** ($\Delta\Delta G < 0$), which was caused by the quite short lifetime ($5.6 \times 10^{-15}, 9.1 \times 10^{-15}, 7.7 \times 10^{-14}$ and $2.2 \times 10^{-14} \text{ s}$) for the **1↔20, 6↔23, 28↔43** and **31↔44** conformational transitions (Table 3). However, at their immersion into the solution with the dielectric permittivity $\epsilon = 4$, which corresponded to the interfaces of the biomolecular interactions [16,17], they became dynamically stable with a lifetime 10^{-12} s ($2.8 \times 10^{-12}, 5.5 \times 10^{-12}, 4.6 \times 10^{-12}$ and $2.7 \times 10^{-12} \text{ s}$, accordingly).

We also explored interconversions of the enantiomers (two stereoisomers, right (R) and left (L), that are mirror reflections of each other) of the non-planar conformers with C_1 point symmetry—**13–18, 20, 23, 24, 26, 29, 30** and **37–48** (Figure 4, Table 4). Enantiomers, as it is known, had the same scalar physico-chemical properties and differed only by the spatial orientation of the dipole moments.

It is quite interesting to consider the structural mechanisms of the interconversion of the enantiomers of the non-planar conformers of the quercetin molecule.

We revealed that the above-mentioned enantiomers could mutually interconvert by the two different pathways from the energetical and topological points of view: first, through the quasi-planar

TS and second, through the mirror-symmetric torsional motion of the O3H hydroxyl group through the corresponding planar conformers (with O3H...O4 and C2'/C6'H...O3 H-bond [16]) as intermediate.

Comparison of the activation energy of Gibbs free energies of these two pathways of interconversion indicate that enantiomers of the non-planar conformers of the quercetin molecule most probably mutually interconvert according to the first mechanism—through the quasi-planar TSs with C_1 point symmetry ($\text{HO}3\text{C}3\text{C}2\text{C}1 = \pm(11.0\text{--}19.1)$, $\text{HC}2'/\text{C}6'\text{C}1'\text{C}2 = \pm(0.6\text{--}2.9)$ and $\text{C}3\text{C}2\text{C}1'\text{C}2'/\text{C}3\text{C}2\text{C}1'\text{C}6' = \pm(1.7\text{--}9.1)$ degree; $\Delta\Delta G_{\text{TS}} = 1.65\text{--}5.59 \text{ kcal}\cdot\text{mol}^{-1}$; Table 4). This effect was caused by the great structural flexibility of the molecule: there were low-frequency ($\nu < 100 \text{ cm}^{-1}$) modes in its vibrational spectra, corresponding to the motions of the (A + C) and B rings around the C2–C1' bond.

We established that the processes of the interconversion of the significantly non-planar enantiomers ($\text{C}3\text{C}2\text{C}1'\text{C}2'/\text{C}6' 42\text{--}44$ degree [16]) occurred through the rearrangement of the (A + C) and B rings of the quercetin molecule into the quasi-planar structures. TSs of these transitions had quasi-planar architecture ($\text{HO}3\text{C}3\text{C}2\text{C}1 = \pm(11.0\text{--}19.1)$; $\text{HC}2'/\text{C}6'\text{C}1'\text{C}2 = \pm(0.6\text{--}2.9)$; $\text{C}3\text{C}2\text{C}1'\text{C}2'/\text{C}3\text{C}2\text{C}1'\text{C}6' = \pm(1.7\text{--}9.1)$ degree) and were characterized by the imaginary frequencies, which were in the range $221.3\text{--}347.9 \text{ cm}^{-1}$. Gibbs free energy barriers for these reactions were quite low ($1.65\text{--}5.59 \text{ kcal mol}^{-1}$), that is they were proceeding quite easily ($\tau_{99.9\%} = 8.52 \times 10^{-12}\text{--}6.46 \times 10^{-9} \text{ s}$; Table 4).

By following the IRC calculations, we established that firstly it occurs by the moving of the O3H hydroxyl groups and C2'H/C6'H groups of the B ring in the opposite directions, followed by the rearrangement of (A + C) and B rings via the rotation around the C2–C1' bond, leading to the decreasing of their dihedral angles (Table 4). At this, the intramolecular O3H ... C2'H/C6'H H-bonds between the (A + C) and B rings switch into the dihydrogen O3H ... HC2'/C6' H-bonds ($4.58\text{--}4.78/4.70\text{--}4.84 \text{ kcal mol}^{-1}$). At this new intramolecular unusual C2'/C6' ... O1 H-bond ($4.67\text{--}4.73/4.63\text{--}4.70 \text{ kcal mol}^{-1}$) also arose. Notably, at these transformations the C3C2C1' and C2'/C6'C1'C2 angles increased ($126\rightarrow130$ and $122\rightarrow125$ degrees, respectively) in order to enable the arrangement of the (A + C) and B rings and O3H and C2'H/C6'H hydroxyl groups in the plane. Earlier such H-bonds have been observed in the dozens of the prototropic tautomers, which are isomers differing by the positions of the protons and π -electrons [49], of the quercetin molecule [50]. Their characteristic property is the unusual range of angles of the C2'H/C6'H ... O1 H-bonding = $98.1\text{--}99.9$ degree (Table 5).

It is interesting to note, that planar structures with zero values of the $\text{HO}3\text{C}3\text{C}2\text{C}1$, $\text{HC}2'/\text{C}6'\text{C}1'\text{C}2$ and $\text{C}3\text{C}2\text{C}1'\text{C}2'/\text{C}3\text{C}2\text{C}1'\text{C}6'$ angles (point symmetry C_s) were characterized by the presence of the two imaginary frequencies ($19.5\text{--}40.2$ and $466.1\text{--}538.6 \text{ cm}^{-1}$), had higher Gibbs free energies ($0.69\text{--}1.53 \text{ kcal mol}^{-1}$) than quasi-planar TSs, while close values of the dipole moment, and they should be considered as so-called TSs between the just-mentioned non-planar TSs, which control interconversion of the enantiomers of the quercetin molecule (Figure 4 and Table 4).

We are convinced that obtained by us data according the structurally symmetrical mechanisms of the interconversion of the enantiomers of the 24 non-planar conformers of the quercetin molecule are quite important for the understanding of the nature of the stereo-specific interaction of this legendary molecule with molecular targets.

Table 1. Energetic, polar, structural and kinetic characteristics of the conformational transitions in the isolated quercetin molecule via the mirror-symmetrical rotations of the O7H hydroxyl group around the C7–O7 bond through the transition states with a non-perpendicularly oriented O7H group, obtained at the MP2/6-311++G(2df,pd)//B3LYP/6-311++G(d,p) level of quantum-mechanical (QM) theory under standard conditions (see Figure 1).

Conformational Transition	μ_{TS}^a	ν_i^b	ΔG^c	ΔE^d	$\Delta\Delta G_{TS}^e$	$\Delta\Delta E_{TS}^f$	$\Delta\Delta G^g$	$\Delta\Delta E^h$	k_f^i	k_r^j	$\tau_{99.9\%}^k$	τ^l	$HO7C7C8/HO7C7C6^m$
1↔5	2.52	401.5	0.34	0.32	4.12	4.59	3.78	4.27	6.72×10^9	1.20×10^{10}	3.70×10^{-10}	8.36×10^{-11}	±90.6
2↔4	4.69	405.4	0.08	0.23	4.27	4.56	4.19	4.32	5.23×10^9	5.99×10^9	6.16×10^{-10}	1.67×10^{-10}	±90.8
3↔6	4.57	400.9	0.28	0.53	4.11	4.63	3.83	4.10	6.87×10^9	1.10×10^{10}	3.86×10^{-10}	9.07×10^{-11}	±89.9
7↔8	6.11	401.0	0.34	0.37	3.88	4.59	3.54	4.22	1.01×10^{10}	1.79×10^{10}	2.46×10^{-10}	5.59×10^{-11}	±90.3
9↔11	2.87	401.1	0.22	0.50	4.24	4.62	4.02	4.12	5.48×10^9	8.00×10^9	5.12×10^{-10}	1.25×10^{-10}	±90.1
10↔12	3.74	400.3	0.38	0.39	4.08	4.60	3.71	4.22	7.17×10^9	1.34×10^{10}	3.35×10^{-10}	7.45×10^{-11}	±90.3
13↔23	6.44	395.1	3.97	4.04	3.98	4.52	0.01	0.48	8.50×10^9	6.94×10^{12}	9.94×10^{-13}	1.44×10^{-13}	±89.9
14↔17	7.92	399.3	0.35	0.36	3.98	4.52	3.63	4.16	8.57×10^9	1.54×10^{10}	2.88×10^{-10}	6.49×10^{-11}	±90.4
15↔18	8.47	397.0	0.42	0.47	3.98	4.50	3.56	4.03	8.61×10^9	1.75×10^{10}	2.65×10^{-10}	5.72×10^{-11}	±90.1
16↔20	5.63	395.5	2.93	2.95	3.61	4.14	0.68	1.19	1.59×10^{10}	2.24×10^{12}	3.06×10^{-12}	4.47×10^{-13}	±90.3
19↔25	2.54	385.9	0.60	0.79	3.78	4.40	3.18	3.61	1.19×10^{10}	3.28×10^{10}	1.55×10^{-10}	3.05×10^{-11}	±93.0
21↔31	2.26	385.4	0.74	0.88	3.91	4.38	3.17	3.50	9.62×10^9	3.36×10^{10}	1.60×10^{-10}	2.98×10^{-11}	±93.3
22↔28	5.82	382.5	0.49	0.51	3.78	4.17	3.24	3.66	1.18×10^{10}	2.95×10^{10}	1.67×10^{-10}	3.39×10^{-11}	±92.3
24↔29	5.73	396.2	0.46	0.51	3.99	4.52	3.53	4.01	8.46×10^9	1.84×10^{10}	2.57×10^{-10}	5.43×10^{-11}	±93.3
26↔30	4.82	395.0	0.45	0.44	4.02	4.53	3.57	4.08	7.93×10^9	1.70×10^{10}	2.77×10^{-10}	5.88×10^{-11}	±90.2
27↔32	5.97	385.0	0.59	0.62	3.79	4.16	3.20	3.55	1.16×10^{10}	3.14×10^{10}	1.61×10^{-10}	3.18×10^{-11}	±92.7
33↔35	4.77	385.2	0.57	0.64	3.77	4.20	3.20	3.56	1.20×10^{10}	3.16×10^{10}	1.58×10^{-10}	3.16×10^{-11}	±92.8
34↔36	3.32	383.2	0.58	0.60	3.78	4.17	3.20	3.57	1.18×10^{10}	3.16×10^{10}	1.59×10^{-10}	3.17×10^{-11}	±92.5
37↔43	5.89	378.4	2.62	2.71	3.51	3.97	0.89	1.26	1.87×10^{10}	1.56×10^{12}	4.37×10^{-12}	6.40×10^{-13}	±92.3
38↔41	3.94	379.3	0.46	0.66	3.63	4.15	3.17	3.49	1.53×10^{10}	3.33×10^{10}	1.42×10^{-10}	3.00×10^{-11}	±92.8
39↔44	5.49	381.7	2.79	2.95	3.65	4.18	0.86	1.23	1.47×10^{10}	1.63×10^{12}	4.20×10^{-12}	6.13×10^{-13}	±92.8
40↔42	7.02	378.0	0.43	0.58	3.53	4.05	3.10	3.46	1.80×10^{10}	3.72×10^{10}	1.25×10^{-10}	2.69×10^{-11}	±92.6
45↔47	4.33	379.3	0.42	0.54	3.54	4.03	3.12	3.49	1.78×10^{10}	3.63×10^{10}	1.28×10^{-10}	2.76×10^{-11}	±92.5
46↔48	5.03	445.0	0.43	0.61	3.57	4.10	3.14	3.49	1.68×10^{10}	3.48×10^{10}	1.34×10^{-10}	2.88×10^{-11}	±92.7

^a The dipole moment of the transition state (TS), Debye. ^b The imaginary frequency at the TS of the conformational transition, cm^{-1} . ^c The Gibbs free energy of the initial relatively the terminal conformer of the quercetin molecule ($T = 298.15 \text{ K}$), $\text{kcal}\cdot\text{mol}^{-1}$. ^d The electronic energy of the initial relatively the terminal conformer of the quercetin molecule, $\text{kcal}\cdot\text{mol}^{-1}$. ^e The Gibbs free energy barrier for the forward conformational transformation of the quercetin molecule, $\text{kcal}\cdot\text{mol}^{-1}$. ^f The electronic energy barrier for the forward conformational transformation of the quercetin molecule, $\text{kcal}\cdot\text{mol}^{-1}$. ^g The Gibbs free energy barrier for the reverse conformational transformation of the quercetin molecule, $\text{kcal}\cdot\text{mol}^{-1}$. ^h The electronic energy barrier for the reverse conformational transformation of the quercetin molecule, $\text{kcal}\cdot\text{mol}^{-1}$. ⁱ The rate constant for the forward conformational transformation, s^{-1} . ^j The rate constant for the reverse conformational transformation, s^{-1} . ^k The time necessary to reach 99.9% of the equilibrium concentration between the reactant and the product of the reaction of the conformational transformation, s . ^l The lifetime of the product of the conformational transition, s . ^m The dihedral angle, which describes at the TS the orientation of the O7H hydroxyl group relatively the A ring of the quercetin molecule, degree; signs “±” correspond to enantiomers.

Table 2. Energetic, polar, structural and kinetic characteristics of the conformational transitions in the isolated quercetin molecule via the mirror-symmetrical rotations of the O5H hydroxyl group around the C5–O5 bond through the transition states with a non-perpendicularly oriented O5H group, obtained at the MP2/6-311++G(2df,pd)//B3LYP/6-311++G(d,p) level of QM theory under standard conditions (see Figure 2) *.

Conformational Transition	μ_{TS}	ν_i	ΔG	ΔE	$\Delta\Delta G_{TS}$	$\Delta\Delta E_{TS}$	$\Delta\Delta G$	$\Delta\Delta E$	k_f	k_r	$\tau_{99.9\%}$	τ	HO5 C5C10^a
1↔25	2.71	445.0	11.68	12.45	14.41	15.69	2.00	2.48	1.96×10^2	2.49×10^{11}	2.77×10^{-11}	4.01×10^{-12}	±110.9
2↔31	1.69	443.5	12.08	12.63	14.85	15.78	2.77	3.15	9.37×10^1	6.80×10^{10}	1.02×10^{-10}	1.47×10^{-11}	±111.0
3↔28	5.85	445.1	11.79	12.66	14.57	15.83	2.78	3.18	1.51×10^2	6.71×10^{10}	1.03×10^{-10}	1.49×10^{-11}	±111.1
4↔21	3.79	462.2	11.26	11.52	14.51	15.24	3.25	3.72	1.69×10^2	3.07×10^{10}	2.25×10^{-10}	3.26×10^{-11}	±109.0
5↔19	2.54	461.0	10.74	11.34	13.86	15.16	3.12	3.82	5.04×10^2	3.81×10^{10}	1.81×10^{-10}	2.62×10^{-11}	±108.9
6↔22	6.20	463.9	11.02	11.62	14.24	15.43	3.28	3.81	2.64×10^2	2.89×10^{10}	2.39×10^{-10}	3.46×10^{-11}	±109.1
7↔32	5.70	445.9	11.62	12.65	14.39	15.80	2.77	3.15	2.08×10^2	6.88×10^{10}	1.00×10^{-10}	1.45×10^{-11}	±111.1
8↔27	7.05	461.7	10.69	11.66	13.87	15.33	3.18	3.66	4.97×10^2	3.44×10^{10}	2.01×10^{-10}	2.90×10^{-11}	±109.1
9↔36	3.38	444.9	11.94	12.69	14.72	15.86	2.78	3.17	1.17×10^2	6.68×10^{10}	1.03×10^{-10}	1.50×10^{-11}	±111.0
10↔35	4.78	445.0	11.57	12.49	14.33	15.67	2.76	3.17	1.92×10^2	5.87×10^{10}	1.18×10^{-10}	1.70×10^{-11}	±111.0
11↔34	3.56	463.5	11.14	11.59	14.38	15.33	3.24	3.74	2.09×10^2	3.12×10^{10}	2.22×10^{-10}	3.21×10^{-11}	±109.0
12↔33	5.13	461.2	10.62	11.46	13.85	15.20	3.23	3.74	5.14×10^2	3.18×10^{10}	2.18×10^{-10}	3.15×10^{-11}	±108.9
13↔43	5.57	446.8	15.81	16.97	16.17	17.79	0.36	0.82	1.01×10^1	3.97×10^{12}	1.74×10^{-12}	2.52×10^{-13}	±114.2
14↔44	4.58	445.9	15.81	16.97	16.16	17.76	0.35	0.79	1.03×10^1	4.06×10^{12}	1.70×10^{-12}	2.46×10^{-13}	±114.3
15↔42	6.47	443.3	13.62	14.79	16.16	17.82	2.54	3.02	1.02×10^1	9.94×10^{10}	6.95×10^{-11}	1.01×10^{-11}	±114.4
16↔38	5.12	458.6	12.66	13.58	15.78	17.26	3.12	3.68	1.96×10^1	3.80×10^{10}	1.82×10^{-10}	2.63×10^{-11}	±112.3
17↔39	7.06	461.6	12.67	13.66	15.83	17.32	3.16	3.67	1.83×10^1	3.59×10^{10}	1.92×10^{-10}	2.79×10^{-11}	±112.3
18↔40	8.61	458.5	12.77	13.74	15.85	17.38	3.07	3.64	1.75×10^1	4.11×10^{10}	1.68×10^{-10}	2.44×10^{-11}	±112.4
20↔41	3.22	443.1	10.19	11.29	12.75	14.35	2.56	3.06	3.24×10^3	9.70×10^{10}	7.12×10^{-11}	1.03×10^{-11}	±114.3
23↔37	7.06	462.6	9.22	10.22	12.34	13.88	3.12	3.66	6.61×10^3	3.78×10^{10}	1.83×10^{-10}	2.64×10^{-11}	±112.3
24↔47	3.71	446.8	13.57	14.72	16.17	17.78	2.60	3.06	1.01×10^1	9.10×10^{10}	7.59×10^{-11}	1.10×10^{-11}	±114.2
26↔48	4.82	440.5	13.56	14.67	16.11	17.73	2.55	3.06	1.12×10^1	9.87×10^{10}	7.00×10^{-11}	1.01×10^{-11}	±114.3
29↔45	5.52	462.1	12.69	13.67	15.84	17.34	3.15	3.67	1.78×10^1	3.62×10^{10}	1.91×10^{-10}	2.76×10^{-11}	±112.3
30↔46	6.33	459.0	12.68	13.62	15.76	17.29	3.08	3.67	2.04×10^1	4.09×10^{10}	1.69×10^{-10}	2.44×10^{-11}	±112.3

* See definitions in the footnote of Table 1. ^a The dihedral angle, which describes at the TS the orientation of the O5H hydroxyl group relatively the A ring of the quercetin molecule, degree.

Table 3. Energetic, polar, structural and kinetic characteristics of the conformational transitions in the isolated quercetin molecule via the mirror-symmetrical rotations of the O3H hydroxyl group around the C3–O3 bond through the transition states with a non-perpendicularly oriented O3H group, obtained at the MP2/6-311++G(2df,pd)//B3LYP/6-311++G(d,p) level of QM theory under standard conditions (see Figure 3) *.

Conformational Transition	μ_{TS}	ν_i	ΔG	ΔE	$\Delta\Delta G_{TS}$	$\Delta\Delta E_{TS}$	$\Delta\Delta G$	$\Delta\Delta E$	k_f	k_r	$\tau_{99.9\%}$	τ	HO3 C3C4 ^a	C3C2 C1'C2'/C3C2 C1'C6' ^b
1↔20	2.77	274.2	11.11	11.40	9.16	9.61	-1.95	-1.80	1.26×10^6	1.78×10^{14}	3.88×10^{-14}	5.61×10^{-15}	±118.6	±32.0
2↔14	5.04	326.5	7.78	7.25	9.53	9.47	1.75	2.21	6.96×10^5	3.54×10^{11}	1.95×10^{-11}	2.83×10^{-12}	±114.1	±31.9
3↔13	5.40	330.4	7.34	7.11	9.20	9.46	1.86	2.35	1.21×10^6	2.95×10^{11}	2.34×10^{-11}	3.39×10^{-12}	±113.8	±29.4
4↔17	7.71	329.3	8.05	7.38	9.85	9.64	1.80	2.26	4.10×10^5	3.29×10^{11}	2.10×10^{-11}	3.04×10^{-12}	±114.3	±32.2
5↔16	5.45	278.6	7.84	8.13	9.19	9.70	1.36	1.57	1.20×10^6	6.70×10^{11}	1.03×10^{-11}	1.49×10^{-12}	±118.6	±32.5
6↔23	7.46	335.1	11.03	10.62	9.38	9.62	-1.65	-0.99	8.99×10^5	1.11×10^{14}	6.22×10^{-14}	9.00×10^{-15}	±113.7	±30.8
7↔15	6.95	324.7	7.06	7.06	9.04	9.32	2.01	2.26	1.59×10^6	2.27×10^{11}	3.04×10^{-11}	4.40×10^{-12}	±113.6	±30.5
8↔18	9.37	328.3	7.14	7.16	9.21	9.53	2.07	2.36	1.19×10^6	2.07×10^{11}	3.34×10^{-11}	4.84×10^{-12}	±113.7	±31.3
9↔24	3.36	328.8	7.49	7.21	9.27	9.49	1.77	2.29	1.08×10^6	3.42×10^{11}	2.02×10^{-11}	2.93×10^{-12}	±114.2	±29.9
10↔26	4.47	284.1	7.54	7.82	9.12	9.51	1.59	1.69	1.36×10^6	4.57×10^{11}	1.51×10^{-11}	2.19×10^{-12}	±117.4	±31.5
11↔29	5.93	333.3	7.73	7.22	9.49	9.54	1.76	2.33	7.49×10^5	3.49×10^{11}	1.98×10^{-11}	2.86×10^{-12}	±114.1	±31.2
12↔30	2.71	288.7	7.61	7.87	9.23	9.66	1.61	1.78	1.14×10^6	4.39×10^{11}	1.57×10^{-11}	2.28×10^{-12}	±117.3	±32.1
19↔38	3.75	301.8	9.76	10.37	11.08	11.98	1.33	1.62	5.00×10^4	7.17×10^{11}	9.64×10^{-12}	1.39×10^{-12}	±118.8	±32.2
21↔39	5.33	351.6	9.46	9.52	11.12	11.74	1.66	2.23	4.80×10^4	4.19×10^{11}	1.65×10^{-11}	2.38×10^{-12}	±114.8	±32.1
22↔37	7.07	359.0	9.23	9.22	11.08	11.74	1.85	2.52	5.19×10^4	3.05×10^{11}	2.26×10^{-11}	3.27×10^{-12}	±114.1	±31.3
25↔41	2.53	298.0	9.62	10.24	11.03	11.85	1.41	1.61	5.41×10^4	6.15×10^{11}	1.12×10^{-11}	1.62×10^{-12}	±118.8	±31.7
27↔40	8.24	346.3	9.22	9.24	11.26	11.63	2.04	2.39	3.80×10^4	2.20×10^{11}	3.14×10^{-11}	4.55×10^{-12}	±114.4	±31.2
28↔43	6.21	354.7	11.36	11.42	10.99	11.68	-0.37	0.26	6.04×10^4	1.30×10^{13}	5.32×10^{-13}	7.70×10^{-14}	±114.2	±29.7
31↔44	1.73	351.6	11.51	11.59	10.39	10.86	-1.12	-0.72	1.64×10^5	4.55×10^{13}	1.52×10^{-13}	2.20×10^{-14}	±114.8	±32.1
32↔42	6.03	343.1	9.06	9.20	11.13	11.58	2.07	2.38	4.69×10^4	2.08×10^{11}	3.33×10^{-11}	4.82×10^{-12}	±114.3	±30.4
33↔46	6.07	310.8	9.67	10.03	11.20	11.79	1.53	1.76	4.10×10^4	5.13×10^{11}	1.35×10^{-11}	1.95×10^{-12}	±117.7	±31.9
34↔45	4.65	356.8	9.28	9.30	10.98	11.65	1.70	2.35	6.15×10^4	3.91×10^{11}	1.77×10^{-11}	2.56×10^{-12}	±114.5	±31.5
35↔48	5.03	307.1	9.53	10.00	11.08	11.74	1.55	1.74	4.99×10^4	4.88×10^{11}	1.42×10^{-11}	2.05×10^{-12}	±117.7	±31.2
36↔47	3.52	352.8	9.12	9.24	10.83	11.56	1.71	2.33	7.88×10^4	3.86×10^{11}	1.79×10^{-11}	2.59×10^{-12}	±113.9	±30.1

* See definitions in the footnote of Table 1. ^a The dihedral angle, which describes at the TS the orientation of the O3H hydroxyl group relatively the C ring of the quercetin molecule, degree.

^b The dihedral angle, which describes the mutual orientation of the (A+C) and B rings of the quercetin molecule accordingly each other, degree.

Table 4. Energetic, polar, structural and kinetic characteristics of the interconversions of the enantiomers of the non-planar conformers of the isolated quercetin molecule via the quasi-planar TSs with C₁ point symmetry, obtained at the MP2/6-311++G(2df,pd)//B3LYP/6-311++G(d,p) level of QM theory under standard conditions (see Figure 4)*.

Interconversion of Enantiomers	μ_{TS}	ν_i	$\Delta\Delta G_{TS}$	$\Delta\Delta E_{TS}$	$k_{f,r}$	$\tau_{99.9\%}$	τ	HO3C3C2C1' ^a	HC2'/C6'C1'C2' ^b	C3C2C1'C2'/C3C2C1'C6' ^c
13 _{R/L} ↔ 13 _{L/R}	5.47	266.3	4.98	5.56	1.48×10^9	2.34×10^{-9}	6.78×10^{-10}	±14.6	±0.7	±7.6
14 _{R/L} ↔ 14 _{L/R}	5.92	256.6	4.01	5.92	7.51×10^9	4.60×10^{-10}	1.33×10^{-10}	±15.7	±0.6	±7.7
15 _{R/L} ↔ 15 _{L/R}	7.31	227.0	5.27	5.68	8.87×10^8	3.89×10^{-9}	1.13×10^{-9}	±18.1	±0.7	±8.4
16 _{R/L} ↔ 16 _{L/R}	6.20	344.0	5.17	6.72	1.11×10^9	3.10×10^{-9}	8.99×10^{-10}	±16.4	±2.9	±7.7
17 _{R/L} ↔ 17 _{L/R}	8.57	250.1	5.21	5.92	9.82×10^8	3.52×10^{-9}	1.02×10^{-9}	±18.0	±0.6	±9.1
18 _{R/L} ↔ 18 _{L/R}	9.79	221.3	5.33	5.82	8.00×10^8	4.32×10^{-9}	1.25×10^{-9}	±19.1	±0.7	±8.7
20 _{R/L} ↔ 20 _{L/R}	3.53	347.9	1.81	3.25	3.22×10^{11}	1.07×10^{-11}	3.11×10^{-12}	±16.2	±2.8	±7.7
23 _{R/L} ↔ 23 _{L/R}	7.69	244.7	1.65	2.31	4.06×10^{11}	8.52×10^{-12}	2.47×10^{-12}	±16.1	±0.6	±8.1
24 _{R/L} ↔ 24 _{L/R}	3.89	268.7	4.96	5.64	1.53×10^9	2.25×10^{-9}	6.52×10^{-10}	±16.0	±0.7	±8.2
26 _{R/L} ↔ 26 _{L/R}	4.73	326.0	5.49	6.50	6.37×10^8	5.43×10^{-9}	1.57×10^{-9}	±15.9	±2.3	±7.7
29 _{R/L} ↔ 29 _{L/R}	6.52	263.7	5.09	5.85	1.22×10^9	2.83×10^{-9}	8.19×10^{-10}	±17.5	±0.7	±8.7
30 _{R/L} ↔ 30 _{L/R}	7.19	322.1	5.54	6.65	5.88×10^8	5.88×10^{-9}	1.70×10^{-9}	±16.1	±2.4	±7.7
37 _{R/L} ↔ 37 _{L/R}	7.17	270.5	5.02	5.65	1.38×10^9	2.51×10^{-9}	7.26×10^{-10}	±12.6	±0.6	±7.0
38 _{R/L} ↔ 38 _{L/R}	4.02	328.0	5.53	6.50	5.98×10^8	5.78×10^{-9}	1.67×10^{-9}	±15.6	±2.3	±8.0
39 _{R/L} ↔ 39 _{L/R}	6.02	282.3	5.04	5.73	1.33×10^9	2.60×10^{-9}	7.53×10^{-10}	±13.4	±0.7	±7.6
40 _{R/L} ↔ 40 _{L/R}	8.61	241.6	5.20	5.67	1.01×10^9	3.43×10^{-9}	9.93×10^{-10}	±14.0	±0.6	±7.2
41 _{R/L} ↔ 41 _{L/R}	2.21	339.2	5.51	6.44	6.27×10^8	5.51×10^{-9}	1.60×10^{-9}	±14.8	±0.7	±7.7
42 _{R/L} ↔ 42 _{L/R}	6.82	256.9	5.13	5.58	1.13×10^9	3.05×10^{-9}	8.82×10^{-10}	±13.1	±0.7	±6.8
43 _{R/L} ↔ 43 _{L/R}	6.12	307.7	2.56	3.25	8.97×10^{10}	3.85×10^{-11}	1.11×10^{-11}	±11.0	±0.7	±6.3
44 _{R/L} ↔ 44 _{L/R}	3.49	287.6	2.78	3.47	6.14×10^{10}	5.62×10^{-11}	1.63×10^{-11}	±13.3	±0.7	±7.6
45 _{R/L} ↔ 45 _{L/R}	4.90	277.7	4.96	5.70	1.53×10^9	2.25×10^{-9}	6.52×10^{-10}	±13.4	±0.7	±7.4
46 _{R/L} ↔ 46 _{L/R}	6.21	312.2	5.59	6.44	5.35×10^8	6.46×10^{-9}	1.87×10^{-9}	±14.8	±1.8	±7.7
47 _{R/L} ↔ 47 _{L/R}	3.40	308.0	4.75	5.56	2.22×10^9	1.56×10^{-9}	4.51×10^{-10}	±12.1	±0.7	±6.9
48 _{R/L} ↔ 48 _{L/R}	4.93	315.5	5.59	6.35	5.35×10^8	6.46×10^{-9}	1.87×10^{-9}	±14.6	±1.7	±1.7

* See definitions in the footnote of Table 1. Subscripts “R” and “L” denotes “Right” and “Left” enantiomers. ^a The dihedral angle, which forms the O3H hydroxyl group accordingly the C ring of the quercetin molecule, degree. ^b The dihedral angle, which forms the C2'H/C6'H groups accordingly the B ring of the quercetin molecule, degree. ^c The dihedral angle, which describes the mutual orientation of the (A+C) and B rings of the quercetin molecule, degree. Signs “±” correspond to enantiomers.

Table 5. Electron-topological, geometrical and energetic characteristics of the intramolecular specific interactions (H-bonds and attractive van der Waals contacts) in the revealed TSs between the quercetin molecule conformers obtained at the B3LYP/6-311++G(d,p) level of QM theory in the continuum with $\epsilon = 1$ (see Figures 1–4 and Tables 1–4).

Transition State	AH···B H-Bond/AH···HB Dihydrogen H-Bond/A···B vdW Contact	$E_{AH\cdots B}/E_{AH\cdots HB}/E_{A\cdots B}$ ^a	ρ ^b	$\Delta\rho$ ^c	$d_{A\cdots B}$ ^d	$d_{H\cdots B}/d_{H\cdots H}$ ^e	$AH\cdots B$ ^f	$C_3C_2C_1'C_6'$ ^g
1	2	3	4	5	6	7	8	9
$TS^{O7H}_{1\leftrightarrow 5}$	O5H...O4	6.42	0.040	0.124	2.659	1.778	147.0	179.5
	O3H...O4	3.24	0.026	0.103	2.625	2.010	118.8	
	C2'H...O3H *	4.07	0.018	0.077	2.879	2.133	123.9	
$TS^{O7H}_{2\leftrightarrow 4}$	O5H...O4	6.45	0.040	0.124	2.658	1.777	147.0	−0.5
	O3H...O4	3.20	0.026	0.103	2.626	2.014	118.7	
	C6'H...O3H *	3.86	0.018	0.073	2.892	2.156	123.3	
$TS^{O7H}_{3\leftrightarrow 6}$	O5H...O4	6.52	0.040	0.124	2.655	1.773	147.0	−3.2
	O3H...O4	3.13	0.026	0.102	2.630	2.020	118.4	
	C6'H...O3H *	3.80	0.017	0.072	2.898	2.163	123.2	
$TS^{O7H}_{7\leftrightarrow 8}$	O5H...O4	6.50	0.040	0.124	2.656	1.775	147.0	177.8
	O3H...O4	3.12	0.026	0.102	2.629	2.021	118.4	
	C2'H...O3H *	3.87	0.018	0.074	2.882	2.156	122.4	
$TS^{O7H}_{9\leftrightarrow 11}$	O5H...O4	6.50	0.040	0.124	2.656	1.774	147.0	−2.4
	O3H...O4	3.14	0.026	0.102	2.629	2.019	118.5	
	C6'H...O3H *	3.80	0.017	0.072	2.895	2.164	122.9	
$TS^{O7H}_{10\leftrightarrow 12}$	O5H...O4	6.44	0.040	0.124	2.658	1.777	147.0	179.1
	O3H...O4	3.21	0.026	0.103	2.626	2.012	118.7	
	C2'H...O3H *	4.03	0.018	0.076	2.885	2.135	124.1	
$TS^{O7H}_{13\leftrightarrow 23}$	O5H...O4	8.24	0.047	0.135	2.604	1.709	148.2	−42.3
	O3H ... C6' *	2.47	0.013	0.046	3.068	2.422	124.0	
$TS^{O7H}_{14\leftrightarrow 17}$	O5H...O4	8.20	0.047	0.135	2.605	1.710	148.2	−43.1
	O3H ... C6' *	2.45	0.013	0.046	3.064	2.426	123.3	
$TS^{O7H}_{15\leftrightarrow 18}$	O5H...O4	8.25	0.047	0.135	2.604	1.709	148.2	137.2
	O3H ... C2' *	2.48	0.013	0.046	3.063	2.413	124.4	
$TS^{O7H}_{16\leftrightarrow 20}$	O5H...O4	8.20	0.047	0.135	2.605	1.710	148.2	137.7
	O3H ... C2' *	2.35	0.012	0.045	3.052	2.467	118.8	

Table 5. Cont.

Transition State	AH···B H-Bond/AH···HB Dihydrogen H-Bond/A···B vdW Contact	$E_{AH\cdots B}/E_{AH\cdots HB}/E_{A\cdots B}$ ^a	ρ ^b	$\Delta\rho$ ^c	$d_{A\cdots B}$ ^d	$d_{H\cdots B}/d_{H\cdots H}$ ^e	$AH\cdots B$ ^f	$C3C2C1'C6'$ ^g
1	2	3	4	5	6	7	8	9
$TS^{O7H}_{19\leftrightarrow 25}$	O5...O4 *	2.91	0.012	0.049	2.765	-	-	
	O3H...O4	4.60	0.032	0.117	2.571	1.923	121.1	179.7
	C2'H...O3H *	3.98	0.018	0.075	2.886	2.141	123.8	
$TS^{O7H}_{21\leftrightarrow 31}$	O5...O4 *	2.92	0.012	0.049	2.764	-	-	
	O3H...O4	4.55	0.032	0.116	2.572	1.926	120.9	-0.1
	C6'H...O3H *	3.76	0.017	0.071	2.901	2.166	123.2	
$TS^{O7H}_{22\leftrightarrow 28}$	O5...O4 *	2.94	0.012	0.049	2.761	-	-	
	O3H...O4	4.46	0.032	0.116	2.575	1.932	120.7	-2.4
	C6'H...O3H *	3.71	0.017	0.070	2.907	2.173	123.2	
$TS^{O7H}_{24\leftrightarrow 29}$	O5H...O4	8.23	0.047	0.135	2.604	1.709	148.2	
	O3H ... C6' *	2.47	0.013	0.046	3.065	2.420	123.9	-42.4
$TS^{O7H}_{26\leftrightarrow 30}$	O5H...O4	8.22	0.047	0.135	2.605	1.710	148.2	
	O3H ... C2' *	2.37	0.012	0.045	3.057	2.457	120.1	137.4
$TS^{O7H}_{27\leftrightarrow 32}$	O5...O4 *	2.93	0.012	0.049	2.762	-	-	
	O3H...O4	4.43	0.031	0.115	2.575	1.934	120.6	178.7
	C2'H...O3H *	3.79	0.017	0.072	2.891	2.165	122.4	
$TS^{O7H}_{33\leftrightarrow 35}$	O5...O4 *	2.92	0.012	0.049	2.764	-	-	
	O3H...O4	4.57	0.032	0.117	2.572	1.925	121.0	179.4
	C2'H...O3H *	3.95	0.018	0.074	2.892	2.143	124.1	
$TS^{O7H}_{34\leftrightarrow 36}$	O5...O4 *	2.93	0.012	0.049	2.762	-	-	
	O3H...O4	4.48	0.032	0.116	2.574	1.931	120.7	-1.7
	C6'H...O3H *	3.71	0.017	0.070	2.903	2.173	122.9	
$TS^{O7H}_{37\leftrightarrow 43}$	O5...O4 *	3.26	0.013	0.055	2.712	-	-	
	O3H ... C6' *	2.44	0.013	0.046	3.079	2.423	124.8	-42.7
$TS^{O7H}_{38\leftrightarrow 41}$	O5...O4 *	3.25	0.013	0.055	2.714	-	-	
	O3H ... C2' *	2.35	0.012	0.045	3.061	2.465	119.7	137.6
$TS^{O7H}_{39\leftrightarrow 44}$	O5...O4 *	3.25	0.013	0.055	2.714	-	-	
	O3H ... C6' *	2.44	0.013	0.046	3.072	2.425	124.0	-43.1

Table 5. Cont.

Transition State	AH···B H-Bond/AH···HB Dihydrogen H-Bond/A···B vdW Contact	$E_{AH\cdots B}/E_{AH\cdots HB}/E_{A\cdots B}$ ^a	ρ ^b	$\Delta\rho$ ^c	$d_{A\cdots B}$ ^d	$d_{H\cdots B}/d_{H\cdots H}$ ^e	$AH\cdots B$ ^f	$C3C2C1'C6'$ ^g
1	2	3	4	5	6	7	8	9
$TS^{O7H}_{40\leftrightarrow 42}$	O5...O4 *	3.26	0.013	0.055	2.713	-	-	
	O3H ... C2' *	2.46	0.013	0.046	3.070	2.415	124.9	137.2
$TS^{O7H}_{45\leftrightarrow 47}$	O5...O4 *	3.26	0.013	0.055	2.713	-	-	
	O3H ... C6' *	2.45	0.013	0.046	3.075	2.422	124.6	-42.7
$TS^{O7H}_{46\leftrightarrow 48}$	O5...O4 *	3.25	0.013	0.055	2.714	-	-	
	O3H ... C2' *	2.36	0.012	0.045	3.065	2.456	120.8	137.3
$TS^{O5H}_{1\leftrightarrow 25}$	O5...O4 *	2.98	0.012	0.045	2.821	-	-	
	O3H...O4	4.60	0.032	0.117	2.571	1.923	121.1	-178.7
	C2'H...O3H *	4.00	0.018	0.075	2.884	2.139	123.8	
$TS^{O5H}_{2\leftrightarrow 31}$	O5...O4 *	2.98	0.012	0.045	2.820	-	-	
	O3H...O4	4.55	0.032	0.116	2.572	1.926	120.9	1.9
	C2'H...O3H *	3.78	0.017	0.072	2.899	2.165	123.2	
$TS^{O5H}_{3\leftrightarrow 28}$	O5...O4 *	2.99	0.012	0.045	2.818	-	-	
	O3H...O4	4.45	0.032	0.116	2.575	1.933	120.7	1.3
	C2'H...O3H *	3.73	0.017	0.071	2.905	2.171	123.2	
$TS^{O5H}_{4\leftrightarrow 21}$	O5...O4 *	2.97	0.012	0.044	2.823	-	-	
	O3H...O4	4.57	0.032	0.116	2.572	1.925	120.9	1.9
	C2'H...O3H *	3.76	0.017	0.071	2.900	2.167	123.1	
$TS^{O5H}_{5\leftrightarrow 19}$	O5...O4 *	2.97	0.012	0.044	2.823	-	-	
	O3H...O4	4.63	0.032	0.117	2.570	1.921	121.1	-178.7
	C2'H...O3H *	3.99	0.018	0.075	2.885	2.139	123.8	
$TS^{O5H}_{6\leftrightarrow 22}$	O5...O4 *	2.99	0.012	0.045	2.820	-	-	
	O3H...O4	4.49	0.032	0.116	2.574	1.930	120.7	1.4
	C6'H...O3H *	3.74	0.017	0.071	2.904	2.169	123.2	
$TS^{O5H}_{7\leftrightarrow 32}$	O5...O4 *	2.99	0.012	0.045	2.818	-	-	
	O3H...O4	4.43	0.031	0.115	2.576	1.934	120.6	-178.4
	C2'H...O3H *	3.80	0.017	0.072	2.889	2.163	122.4	

Table 5. Cont.

Transition State	AH···B H-Bond/AH···HB Dihydrogen H-Bond/A···B vdW Contact	$E_{AH\cdots B}/E_{AH\cdots HB}/E_{A\cdots B}$ ^a	ρ ^b	$\Delta\rho$ ^c	$d_{A\cdots B}$ ^d	$d_{H\cdots B}/d_{H\cdots H}$ ^e	$AH\cdots B$ ^f	$C3C2C1'C6'$ ^g
1	2	3	4	5	6	7	8	9
$TS^{O5H}_{8\leftrightarrow27}$	O5...O4 *	2.99	0.012	0.045	2.821	-	-	
	O3H...O4	4.46	0.032	0.116	2.574	1.932	120.6	-178.3
	C2'H...O3H *	3.80	0.017	0.072	2.889	2.163	122.4	
$TS^{O5H}_{9\leftrightarrow36}$	O5...O4 *	2.99	0.012	0.045	2.819	-	-	
	O3H...O4	4.48	0.032	0.116	2.575	1.931	120.7	1.6
	C6'H...O3H *	3.73	0.017	0.071	2.901	2.171	122.8	
$TS^{O5H}_{10\leftrightarrow35}$	O5...O4 *	2.98	0.012	0.045	2.820	-	-	
	O3H...O4	4.57	0.032	0.116	2.572	1.925	121.0	-178.8
	C2'H...O3H *	3.97	0.018	0.075	2.890	2.142	124.1	
$TS^{O5H}_{11\leftrightarrow34}$	O5...O4 *	2.98	0.012	0.045	2.821	-	-	
	O3H...O4	4.51	0.032	0.116	2.573	1.929	120.8	1.7
	C6'H...O3H *	3.73	0.017	0.071	2.901	2.171	122.9	
$TS^{O5H}_{12\leftrightarrow33}$	O5...O4 *	2.98	0.012	0.045	2.822	-	-	
	O3H...O4	4.60	0.032	0.117	2.571	1.923	121.0	-178.8
	C2'H...O3H *	3.97	0.018	0.075	2.890	2.142	124.1	
$TS^{O5H}_{13\leftrightarrow43}$	O5...O4 *	3.27	0.014	0.050	2.774	-	-	
	O3H ... C6' *	2.45	0.013	0.046	3.075	2.422	124.6	-42.4
$TS^{O5H}_{14\leftrightarrow44}$	O5...O4 *	3.26	0.014	0.049	2.776	-	-	
	O3H ... C6' *	2.44	0.013	0.046	3.071	2.426	123.9	-43.1
$TS^{O5H}_{15\leftrightarrow42}$	O5...O4 *	3.26	0.014	0.049	2.774	-	-	
	O3H ... C2' *	2.48	0.013	0.046	3.067	2.412	124.7	137.6
$TS^{O5H}_{16\leftrightarrow38}$	O5...O4 *	3.24	0.014	0.049	2.780	-	-	
	O3H ... C2' *	2.33	0.012	0.045	3.064	2.470	119.6	137.1
$TS^{O5H}_{17\leftrightarrow39}$	O5...O4 *	3.24	0.014	0.049	2.779	-	-	
	O3H ... C6' *	2.42	0.013	0.045	3.074	2.430	123.8	-43.2
$TS^{O5H}_{18\leftrightarrow40}$	O5...O4 *	3.25	0.014	0.049	2.777	-	-	
	O3H ... C2' *	2.43	0.013	0.045	3.073	2.420	124.7	136.6

Table 5. Cont.

Transition State	AH···B H-Bond/AH···HB Dihydrogen H-Bond/A···B vdW Contact	$E_{AH\cdots B}/E_{AH\cdots HB}/E_{A\cdots B}$ ^a	ρ ^b	$\Delta\rho$ ^c	$d_{A\cdots B}$ ^d	$d_{H\cdots B}/d_{H\cdots H}$ ^e	$AH\cdots B$ ^f	$C3C2C1'C6'$ ^g
1	2	3	4	5	6	7	8	9
$TS^{O5H}_{20\leftrightarrow 41}$	O5...O4 *	3.25	0.014	0.049	2.777	-	-	137.7
	O3H ... C2' *	2.36	0.012	0.045	3.058	2.464	119.6	
$TS^{O5H}_{23\leftrightarrow 37}$	O5...O4 *	3.24	0.014	0.049	2.777	-	-	-43.7
	O3H ... C6' *	2.42	0.013	0.045	3.084	2.431	124.7	
$TS^{O5H}_{24\leftrightarrow 47}$	O5...O4 *	3.25	0.014	0.049	2.775	-	-	-42.5
	O3H ... C6' *	2.48	0.013	0.046	3.072	2.421	124.5	
$TS^{O5H}_{26\leftrightarrow 48}$	O5...O4 *	3.25	0.014	0.049	2.776	-	-	137.6
	O3H ... C2' *	2.38	0.012	0.045	3.062	2.454	120.7	
$TS^{O5H}_{29\leftrightarrow 45}$	O5...O4 *	3.25	0.014	0.049	2.777	-	-	-43.6
	O3H ... C6' *	2.40	0.013	0.045	3.080	2.429	124.4	
$TS^{O5H}_{30\leftrightarrow 46}$	O5...O4 *	3.24	0.014	0.049	2.779	-	-	136.5
	O3H ... C2' *	2.34	0.012	0.045	3.069	2.461	120.8	
$TS^{O3H}_{1\leftrightarrow 20}$	O5H...O4	8.54	0.049	0.136	2.600	1.699	148.7	149.8
	C2'H...O3H *	2.92	0.014	0.050	2.941	2.369	111.3	
$TS^{O3H}_{2\leftrightarrow 14}$	O5H...O4	8.54	0.049	0.136	2.600	1.699	148.7	-31.9
	C2'H...O3H *	2.89	0.014	0.050	2.950	2.376	111.6	
$TS^{O3H}_{3\leftrightarrow 13}$	O5H...O4	8.58	0.049	0.136	2.598	1.697	148.7	-29.4
	C2'H...O3H *	2.99	0.014	0.051	2.948	2.353	113.0	
$TS^{O3H}_{4\leftrightarrow 17}$	O5H...O4	8.31	0.048	0.135	2.605	2.382	111.4	-32.2
	C2'H...O3H *	2.86	0.014	0.049	2.953	1.925	120.9	
$TS^{O3H}_{5\leftrightarrow 16}$	O5H...O4	8.31	0.048	0.135	2.605	1.707	148.6	149.3
	C2'H...O3H *	2.88	0.014	0.050	2.943	2.376	111.0	
$TS^{O3H}_{6\leftrightarrow 23}$	O5H...O4	8.37	0.048	0.135	2.603	1.705	148.6	-30.8
	C6'H...O3H *	2.92	0.014	0.050	2.952	2.368	112.2	
$TS^{O3H}_{7\leftrightarrow 15}$	O5H...O4	8.37	0.048	0.135	148.747	1.698	148.7	150.8
	C2'H...O3H *	2.92	0.014	0.050	2.937	2.365	111.4	
$TS^{O3H}_{8\leftrightarrow 18}$	O5H...O4	8.35	0.048	0.135	2.604	1.705	148.6	150.0
	C2'H...O3H *	2.90	0.014	0.050	2.940	2.374	111.0	

Table 5. Cont.

Transition State	AH···B H-Bond/AH···HB Dihydrogen H-Bond/A···B vdW Contact	$E_{AH\cdots B}/E_{AH\cdots HB}/E_{A\cdots B}$ ^a	ρ ^b	$\Delta\rho$ ^c	$d_{A\cdots B}$ ^d	$d_{H\cdots B}/d_{H\cdots H}$ ^e	$AH\cdots B$ ^f	$C3C2C1'C6'$ ^g
1	2	3	4	5	6	7	8	9
$TS^{O3H}_{9\leftrightarrow 24}$	O5H...O4 C6'H...O3H *	8.57 2.95	0.049 0.014	0.136 0.051	2.599 2.947	1.698 2.361	148.7 112.4	-29.9
$TS^{O3H}_{10\leftrightarrow 26}$	O5H...O4 C2'H...O3H *	8.54 2.94	0.049 0.014	0.136 0.051	2.599 2.943	1.699 2.363	148.7 111.8	150.3
$TS^{O3H}_{11\leftrightarrow 29}$	O5H...O4 C6'H...O3H *	8.35 2.89	0.048 0.014	0.135 0.049	2.604 2.951	1.705 2.376	148.6 111.7	-31.2
$TS^{O3H}_{12\leftrightarrow 30}$	O5H...O4 C2'H...O3H *	8.32 2.91	0.048 0.014	0.135 0.050	2.605 2.945	1.706 2.371	148.6 111.5	149.5
$TS^{O3H}_{19\leftrightarrow 38}$	O5...O4 * C2'H...O3H *	3.19 2.87	0.013 0.014	0.054 0.049	2.723 2.946	- 2.377	- 111.1	149.5
$TS^{O3H}_{21\leftrightarrow 39}$	O5...O4 * C6'H...O3H *	3.18 2.83	0.013 0.014	0.054 0.048	2.724 2.957	- 2.388	- 111.3	-32.1
$TS^{O3H}_{22\leftrightarrow 37}$	O5...O4 * C6'H...O3H *	3.19 2.85	0.013 0.014	0.054 0.049	2.723 2.959	- 2.382	- 111.8	-31.3
$TS^{O3H}_{25\leftrightarrow 41}$	O5...O4 * C2'H...O3H *	3.22 2.91	0.013 0.014	0.054 0.050	2.719 2.943	- 2.370	- 111.4	150.0
$TS^{O3H}_{27\leftrightarrow 40}$	O5...O4 * C2'H...O3H *	3.19 2.87	0.013 0.014	0.054 0.049	2.723 2.944	- 2.380	- 110.9	150.0
$TS^{O3H}_{28\leftrightarrow 43}$	O5...O4 * C6'H...O3H *	3.21 2.93	0.013 0.014	0.054 0.050	2.719 2.954	- 2.364	- 112.7	-29.7
$TS^{O3H}_{31\leftrightarrow 44}$	O5...O4 * C6'H...O3H *	3.18 2.83	0.013 0.014	0.054 0.048	2.724 2.957	- 2.388	- 111.3	-32.1
$TS^{O3H}_{32\leftrightarrow 42}$	O5...O4 * C2'H...O3H *	3.21 2.91	0.013 0.014	0.054 0.050	2.720 2.942	- 2.371	- 111.3	150.9
$TS^{O3H}_{33\leftrightarrow 46}$	O5...O4 * C2'H...O3H *	3.19 2.89	0.013 0.014	0.054 0.050	2.723 2.948	- 2.373	- 111.5	149.7
$TS^{O3H}_{34\leftrightarrow 45}$	O5...O4 * C6'H...O3H *	3.19 2.83	0.013 0.014	0.054 0.048	2.723 2.957	- 2.387	- 111.3	-31.5

Table 5. Cont.

Transition State	AH···B H-Bond/AH···HB Dihydrogen H-Bond/A···B vdW Contact	$E_{AH\cdots B}/E_{AH\cdots HB}/E_{A\cdots B}$ ^a	ρ ^b	$\Delta\rho$ ^c	$d_{A\cdots B}$ ^d	$d_{H\cdots B}/d_{H\cdots H}$ ^e	$AH\cdots B$ ^f	$C3C2C1'C6'$ ^g
1	2	3	4	5	6	7	8	9
TS^{O3H}_{35↔48}	O5...O4 *	3.22	0.013	0.054	2.719	-	-	
	C2'H...O3H *	2.93	0.014	0.050	2.946	2.365	111.9	150.4
TS^{O3H}_{36↔47}	O5...O4 *	3.21	0.013	0.054	2.720	-	-	
	C6'H...O3H *	2.90	0.014	0.050	2.952	2.371	112.1	-30.1
TS_{13R↔13L}	O5H...O4	8.37	0.048	0.135	2.603	1.705	148.4	
	O3H...HC6' *	4.81	0.023	0.075	2.496	1.592	155.4	-7.6
	C2'H...O1 *	4.74	0.019	0.090	2.619	2.218	99.3	
TS_{14R↔14L}	O5H...O4	8.33	0.048	0.135	2.605	1.707	148.4	
	O3H...HC6' *	4.77	0.023	0.075	2.490	1.590	154.6	-7.7
	C2'H...O1 *	4.72	0.019	0.090	2.617	2.234	98.3	
TS_{15R↔15L}	O5H...O4	8.37	0.048	0.135	2.603	1.705	148.4	
	O3H...HC2' *	4.67	0.022	0.074	2.500	1.603	153.9	171.9
	C6'H...O1 *	4.69	0.019	0.089	2.627	2.233	98.9	
TS_{16R↔16L}	O5H...O4	8.09	0.047	0.134	2.610	1.715	148.3	
	O3H...HC2' *	4.67	0.023	0.074	2.502	1.601	155.4	171.2
	C6'H...O1 *	4.66	0.019	0.089	2.631	2.234	99.2	
TS_{17R↔17L}	O5H...O4	8.10	0.047	0.134	2.610	1.714	148.3	
	O3H...HC6' *	4.73	0.023	0.074	2.493	1.600	153.2	-9.1
	C2'H...O1 *	4.71	0.019	0.089	2.621	2.241	98.1	
TS_{18R↔18L}	O5H...O4	8.16	0.047	0.134	2.608	1.712	148.3	
	O3H...HC2' *	4.58	0.022	0.073	2.496	1.612	151.5	170.8
	C6'H...O1 *	4.64	0.019	0.088	2.631	2.239	98.9	
TS_{20R↔20L}	O5H...O4	8.30	0.048	0.135	2.605	1.707	148.4	
	O3H...HC2' *	4.68	0.023	0.074	2.502	1.600	155.5	171.3
	C6'H...O1 *	4.69	0.019	0.089	2.629	2.231	99.2	
TS_{23R↔23L}	O5H...O4	8.18	0.047	0.134	2.608	1.712	148.3	
	O3H...HC6' *	4.78	0.023	0.075	2.493	1.595	154.2	-8.1
	C2'H...O1 *	4.69	0.019	0.089	2.624	2.223	99.2	

Table 5. Cont.

Transition State	AH···B H-Bond/AH···HB Dihydrogen H-Bond/A···B vdW Contact	$E_{AH\cdots B}/E_{AH\cdots HB}/E_{A\cdots B}$ ^a	ρ ^b	$\Delta\rho$ ^c	$d_{A\cdots B}$ ^d	$d_{H\cdots B}/d_{H\cdots H}$ ^e	$AH\cdots B$ ^f	$C3C2C1'C6'$ ^g
1	2	3	4	5	6	7	8	9
TS_{24R↔24L}	O5H...O4	8.36	0.048	0.135	2.603	1.705	148.4	
	O3H...HC6' *	4.77	0.023	0.075	2.497	1.597	154.8	8.2
	C2'H...O1 *	4.71	0.019	0.089	2.624	2.219	99.5	
TS_{26R↔26L}	O5H...O4	8.32	0.048	0.135	2.605	1.707	148.4	
	O3H...HC2' *	4.70	0.023	0.074	2.499	1.597	155.3	171.4
	C6'H...O1 *	4.70	0.019	0.089	2.626	2.235	98.8	
TS_{29R↔29L}	O5H...O4	8.16	0.047	0.134	2.608	1.712	148.3	
	O3H...HC6' *	4.76	0.023	0.075	2.497	1.597	154.6	-8.2
	C2'H...O1 *	4.67	0.019	0.089	2.627	2.223	99.5	
TS_{30R↔30L}	O5H...O4	8.11	0.047	0.134	2.610	1.714	148.3	
	O3H...HC2' *	4.69	0.023	0.074	2.499	1.598	155.1	171.3
	C6'H...O1 *	4.66	0.019	0.089	2.629	2.238	98.8	
TS_{37R↔37L}	O5...O4 *	3.20	0.013	0.054	2.722	-	-	
	O3H...HC6' *	4.82	0.023	0.075	2.501	1.591	156.8	-7.0
	C2'H...O1 *	4.68	0.019	0.089	2.624	2.221	99.4	
TS_{38R↔38L}	O5...O4 *	13.75	0.047	0.134	2.725	-	-	
	O3H...HC2' *	4.67	0.023	0.074	2.507	1.602	156.0	171.2
	C6'H...O1 *	4.66	0.019	0.089	2.633	2.235	99.3	
TS_{39R↔39L}	O5...O4 *	3.17	0.013	0.054	2.726	-	-	
	O3H...HC6' *	4.80	0.023	0.075	2.502	1.593	156.6	-7.6
	C2'H...O1 *	4.70	0.019	0.089	2.621	2.236	98.4	
TS_{40R↔40L}	O5...O4 *	3.19	0.013	0.054	2.723	-	-	
	O3H...HC2' *	4.69	0.023	0.074	2.505	1.601	155.6	-172.5
	C6'H...O1 *	4.63	0.019	0.088	2.631	2.235	99.1	
TS_{41R↔41L}	O5...O4 *	3.20	0.013	0.054	2.722	-	-	
	O3H...HC2' *	4.68	0.023	0.074	2.507	1.599	156.6	171.6
	C6'H...O1 *	4.66	0.019	0.088	2.631	2.232	99.3	

Table 5. Cont.

Transition State	AH···B H-Bond/AH···HB Dihydrogen H-Bond/A···B vdW Contact	$E_{AH\cdots B}/E_{AH\cdots HB}/E_{A\cdots B}$ ^a	ρ ^b	$\Delta\rho$ ^c	$d_{A\cdots B}$ ^d	$d_{H\cdots B}/d_{H\cdots H}$ ^e	$AH\cdots B$ ^f	$C3C2C1'C6'$ ^g
1	2	3	4	5	6	7	8	9
TS_{42R↔42L}	O5...O4 *	3.21	0.013	0.054	2.720	-	-	
	O3H...HC2' *	4.71	0.023	0.074	2.506	1.600	156.3	-172.9
	C6'H...O1 *	4.67	0.019	0.089	2.628	2.232	99.1	
TS_{43R↔43L}	O5...O4 *	3.21	0.013	0.054	2.720	-	-	
	O3H...HC6' *	4.84	0.023	0.075	2.503	1.589	157.8	6.3
	C2'H...O1 *	4.73	0.019	0.090	2.620	2.216	99.4	
TS_{44R↔44L}	O5...O4 *	3.20	0.013	0.054	2.722	-	-	
	O3H...HC6' *	4.84	0.023	0.075	2.500	1.591	156.8	7.6
	C2'H...O1 *	4.71	0.019	0.090	2.620	2.236	98.3	
TS_{45R↔45L}	O5...O4 *	3.19	0.013	0.054	2.723	-	-	
	O3H...HC6' *	4.79	0.023	0.075	2.504	1.595	156.7	7.5
	C2'H...O1 *	4.66	0.019	0.088	2.628	2.221	99.6	
TS_{46R↔46L}	O5...O4 *	3.18	0.013	0.054	2.724	-	-	
	O3H...HC2' *	4.69	0.023	0.074	2.503	1.598	156.0	171.6
	C6'H...O1 *	4.63	0.019	0.088	2.631	2.238	98.9	
TS_{47R↔47L}	O5...O4 *	3.21	0.013	0.054	2.720	-	-	
	O3H...HC6' *	4.81	0.023	0.075	2.505	1.592	157.6	6.9
	C2'H...O1 *	4.70	0.019	0.089	2.625	2.216	99.7	
TS_{48R↔48L}	O5...O4 *	3.20	0.013	0.054	2.721	-	-	
	O3H...HC2' *	4.70	0.023	0.074	2.503	1.598	156.2	171.7
	C6'H...O1 *	4.66	0.019	0.089	2.628	2.235	98.9	

^a Energy of the AH···B/AH···HB/A···B specific contact, calculated by Espinosa–Molins–Lecomte (Espinosa, Molins and Lecomte, 1998; Mata, Alkorta, Espinosa and Molins, 2011; marked with an asterisk) or Nikolaienko–Bulavin–Hovorun (Nikolaienko, Bulavin and Hovorun, 2011) formulas, kcal·mol⁻¹. ^b The electron density at the (3, -1) BCP of the specific contact, a.u.

^c The Laplacian of the electron density at the (3, -1) BCP of the specific contact, a.u. ^d The distance between the A and B atoms of the AH···B/A···B specific contact, Å. ^e The distance between the H and B/H atoms of the AH···B/AH···HB specific contact, Å. ^f The H-bond angle, degree. ^g Dihedral angle between the (A + C) and B rings, degree.

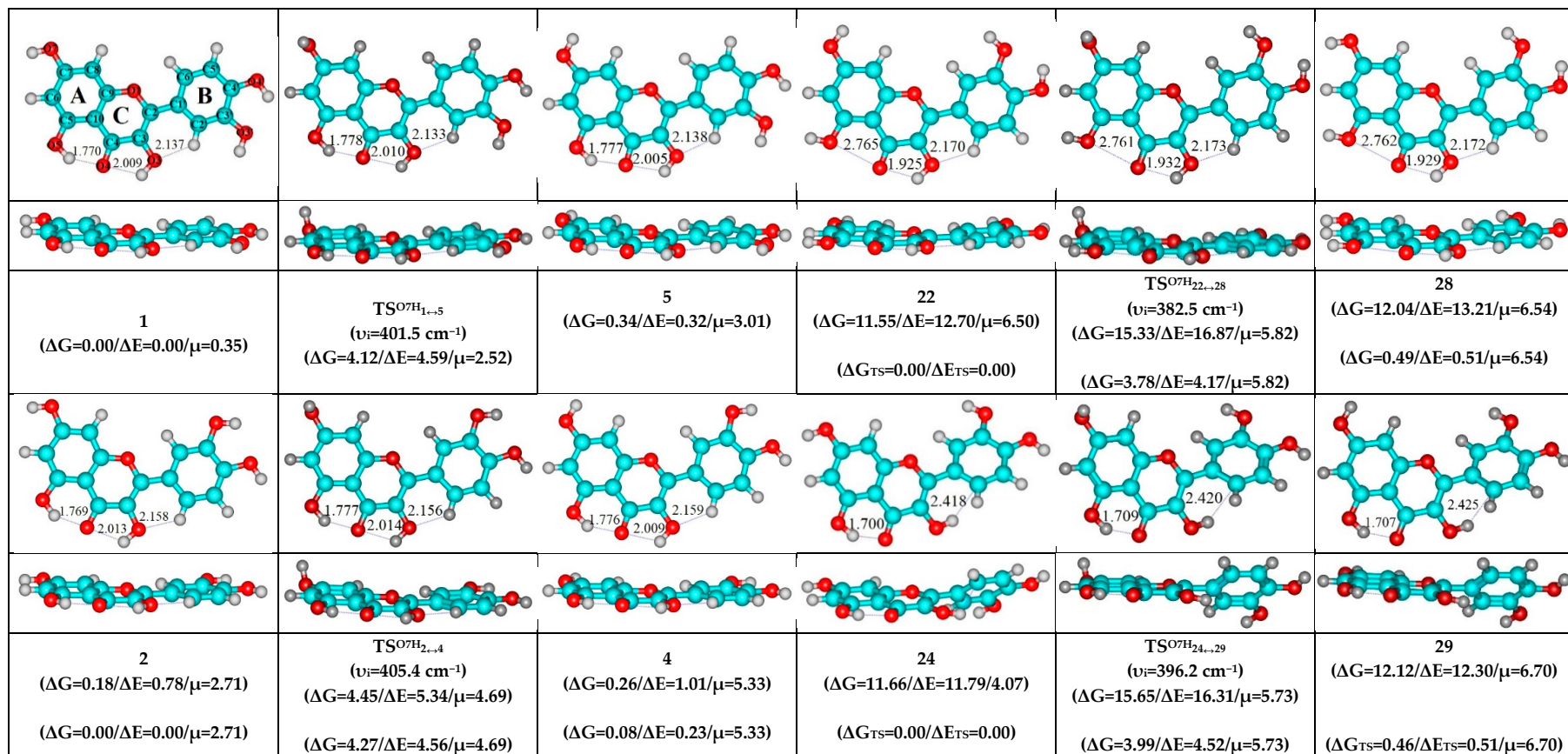


Figure 1. Cont.

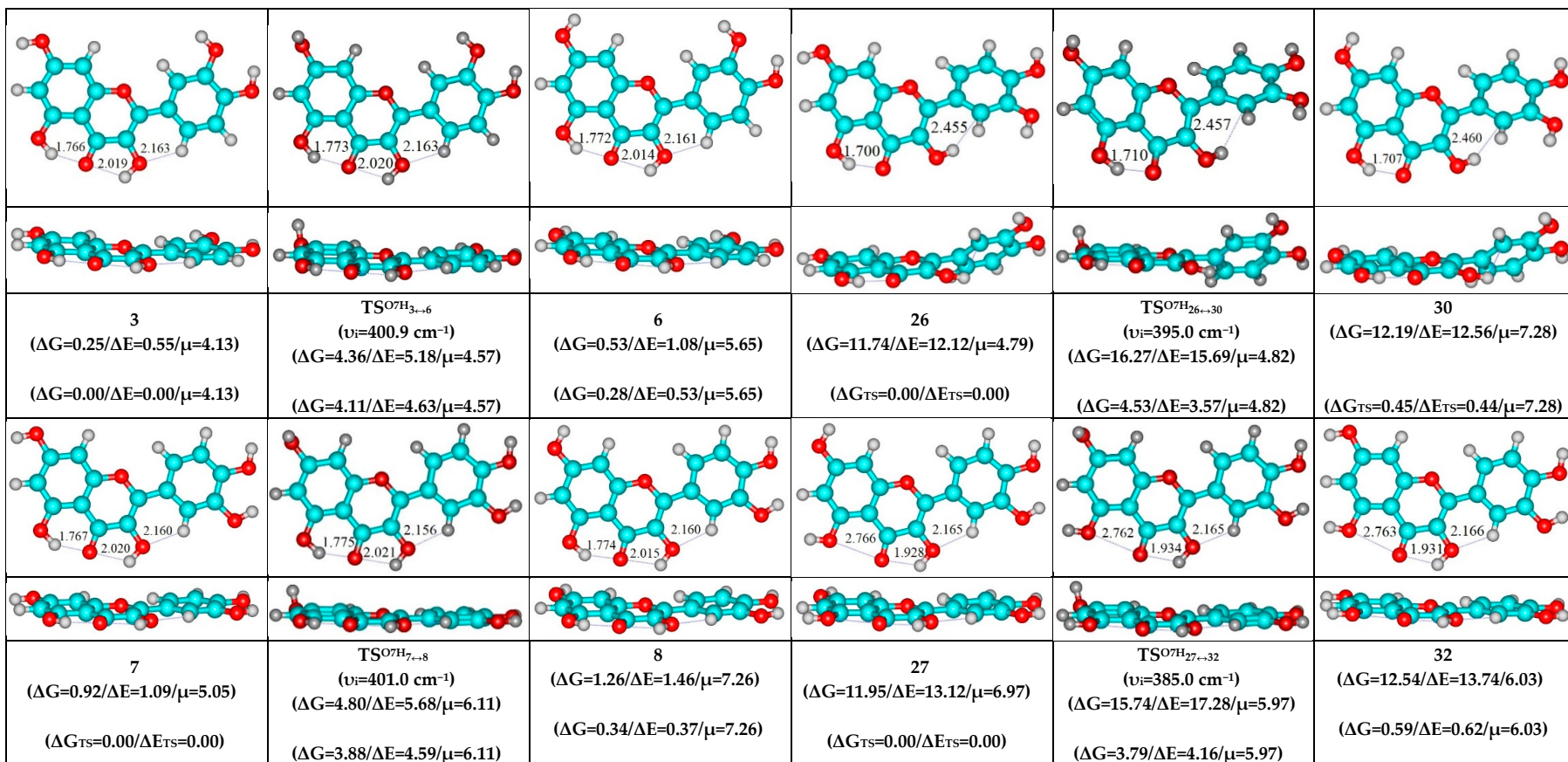


Figure 1. Cont.

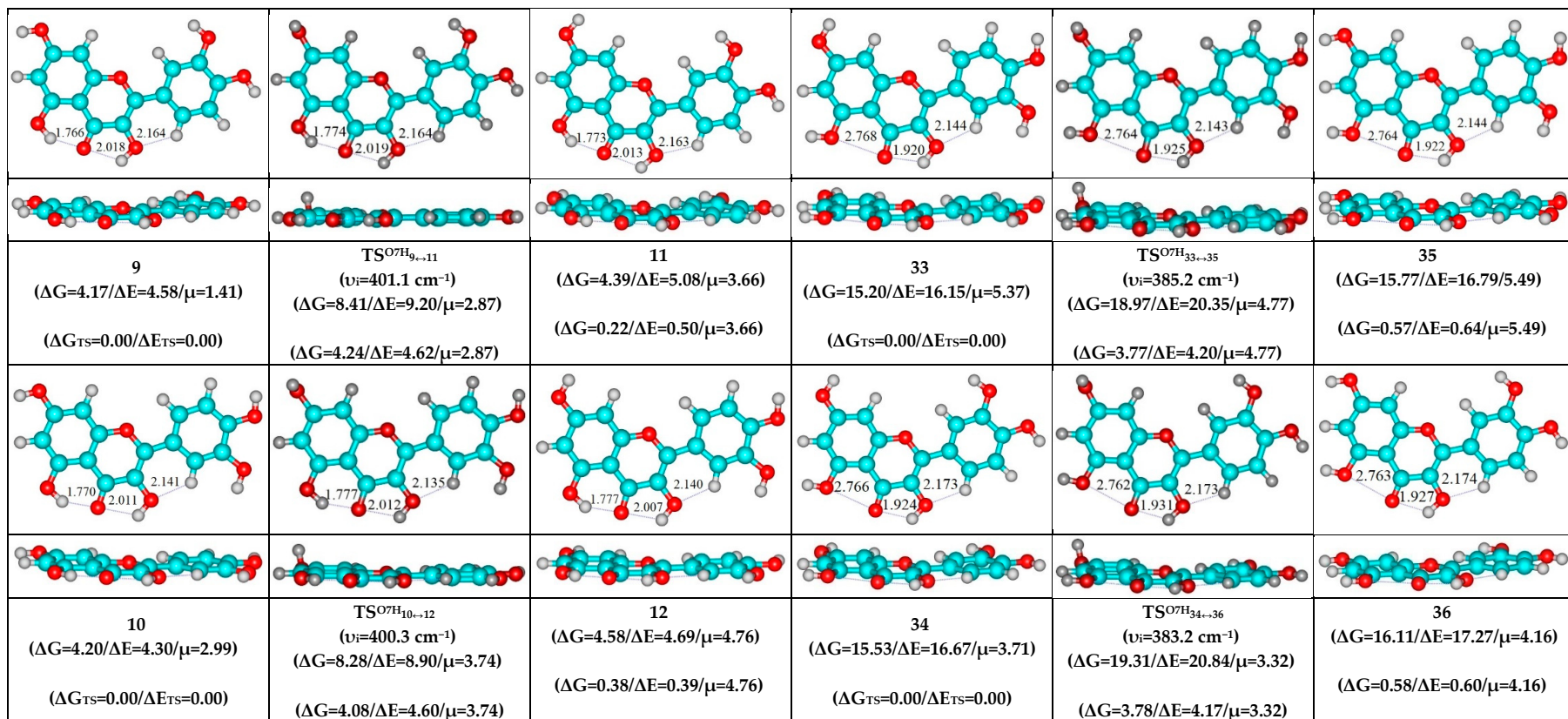


Figure 1. Cont.

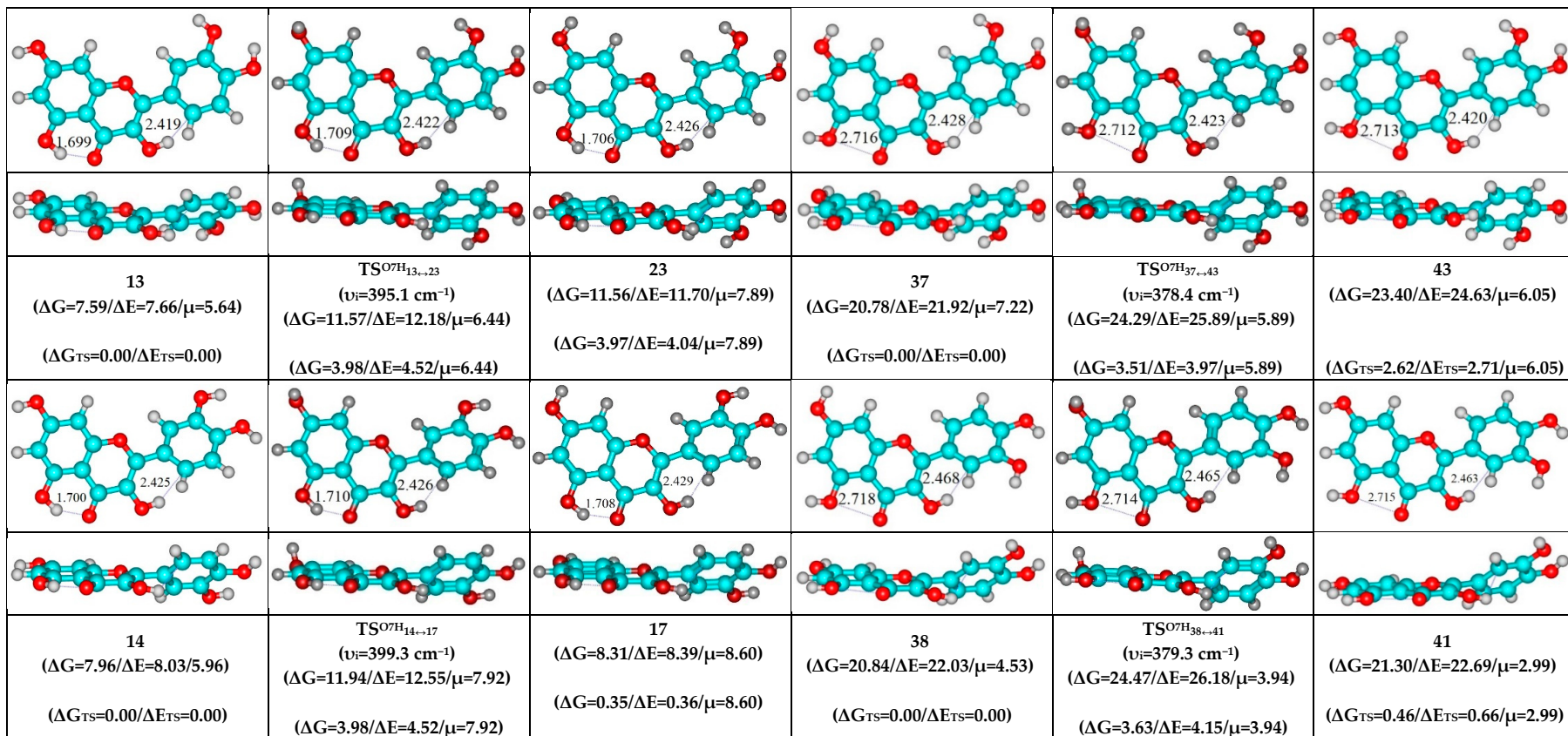


Figure 1. Cont.

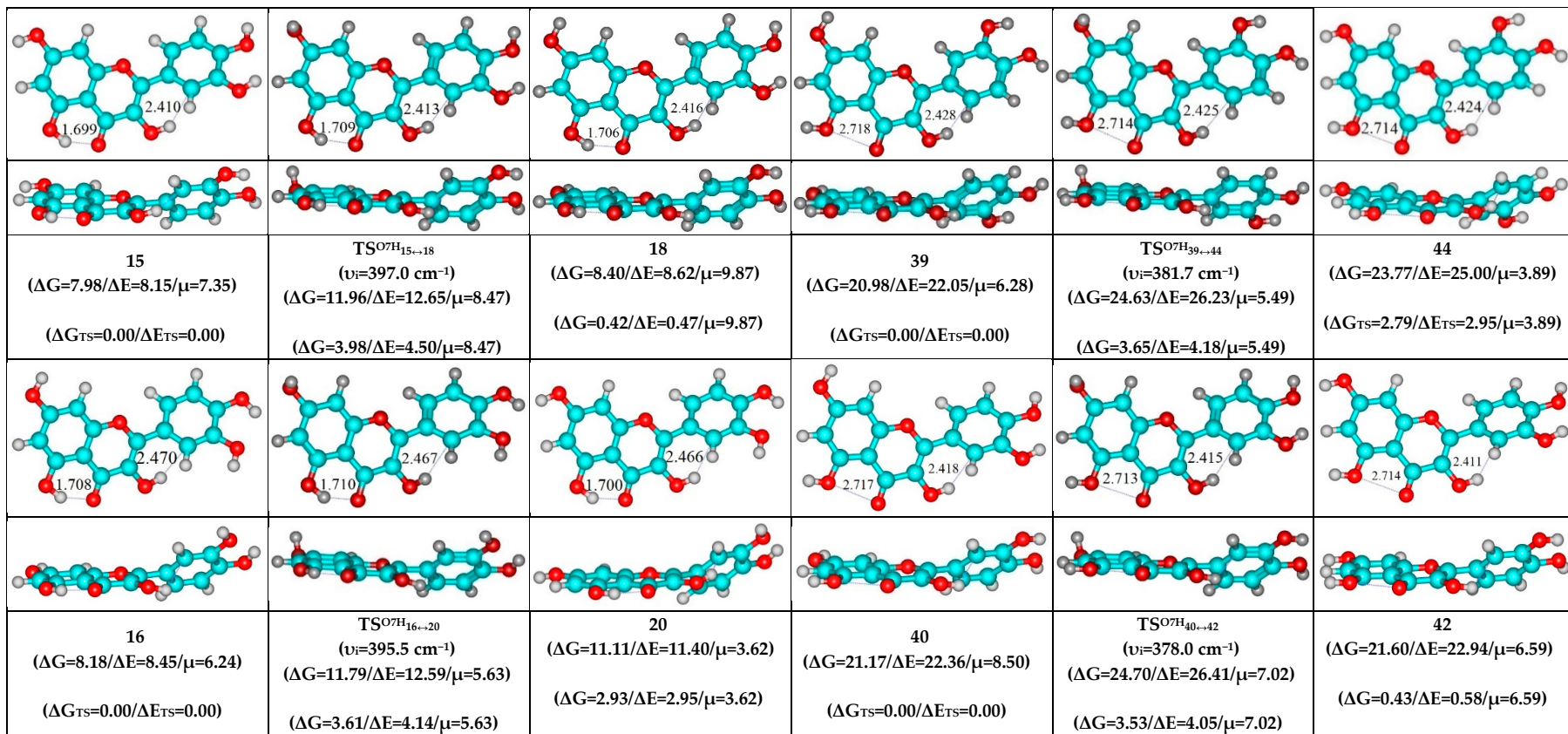


Figure 1. Cont.

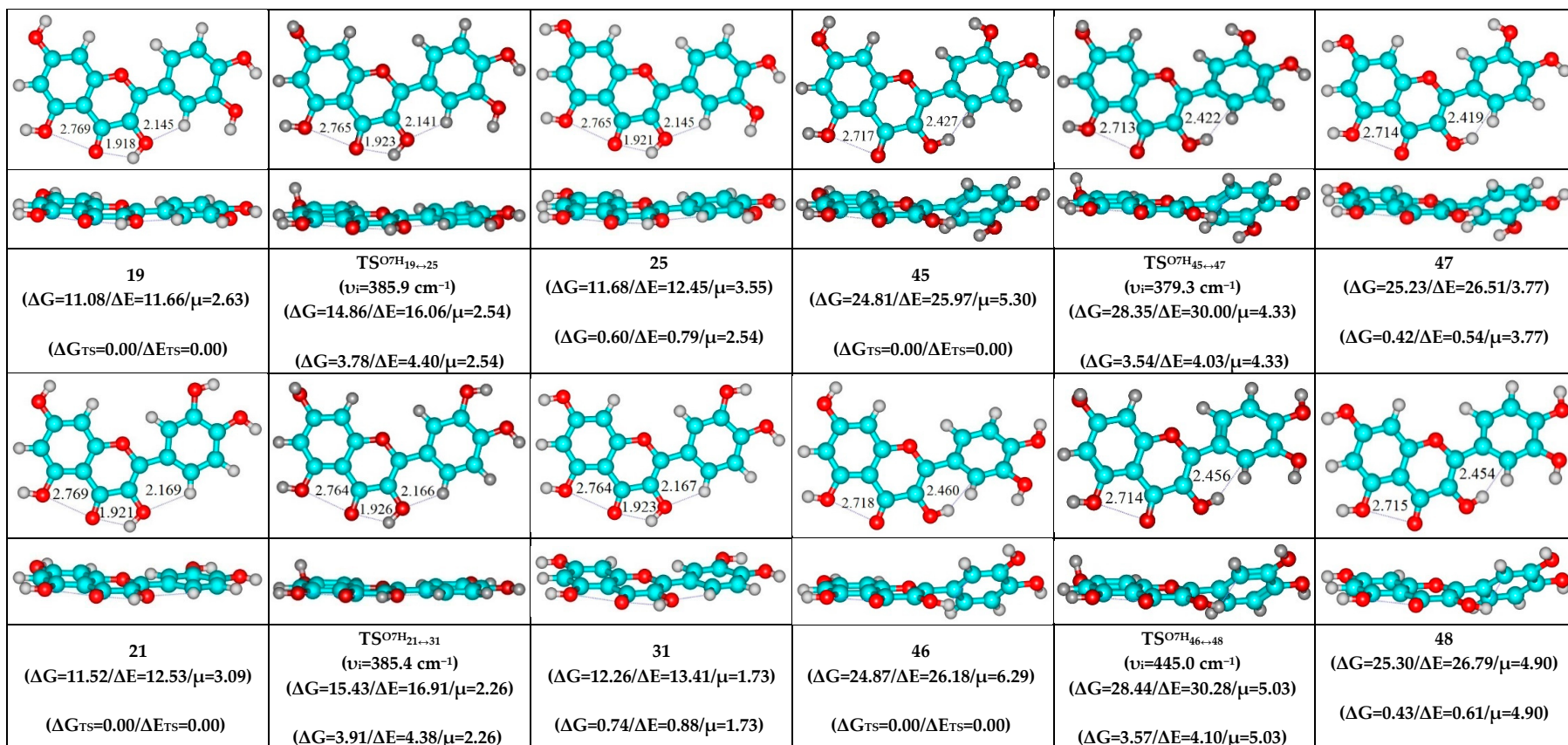


Figure 1. Geometrical structures of the quercetin molecule conformers and TSs with a non-perpendicularly oriented hydroxyl groups of their mutual interconversions via the mirror-symmetrical rotation of the O7H hydroxyl groups around the C7–O7 bonds, obtained at the MP2/6-311++G(2df,pd)//B3LYP/6-311++G(d,p) level of QM theory under standard conditions. Relative Gibbs free ΔG and electronic ΔE energies (in $\text{kcal}\cdot\text{mol}^{-1}$) (upper row represents energies relatively the conformer 1, while lower row—relatively the initial conformer for each transformation), dipole moments μ (Debye) and imaginary frequencies at TSs are provided at the MP2/6-311++G(2df,pd)//B3LYP/6-311++G(d,p) level of theory). Dotted lines indicate specific intramolecular contacts; their lengths are presented in Angstrom.

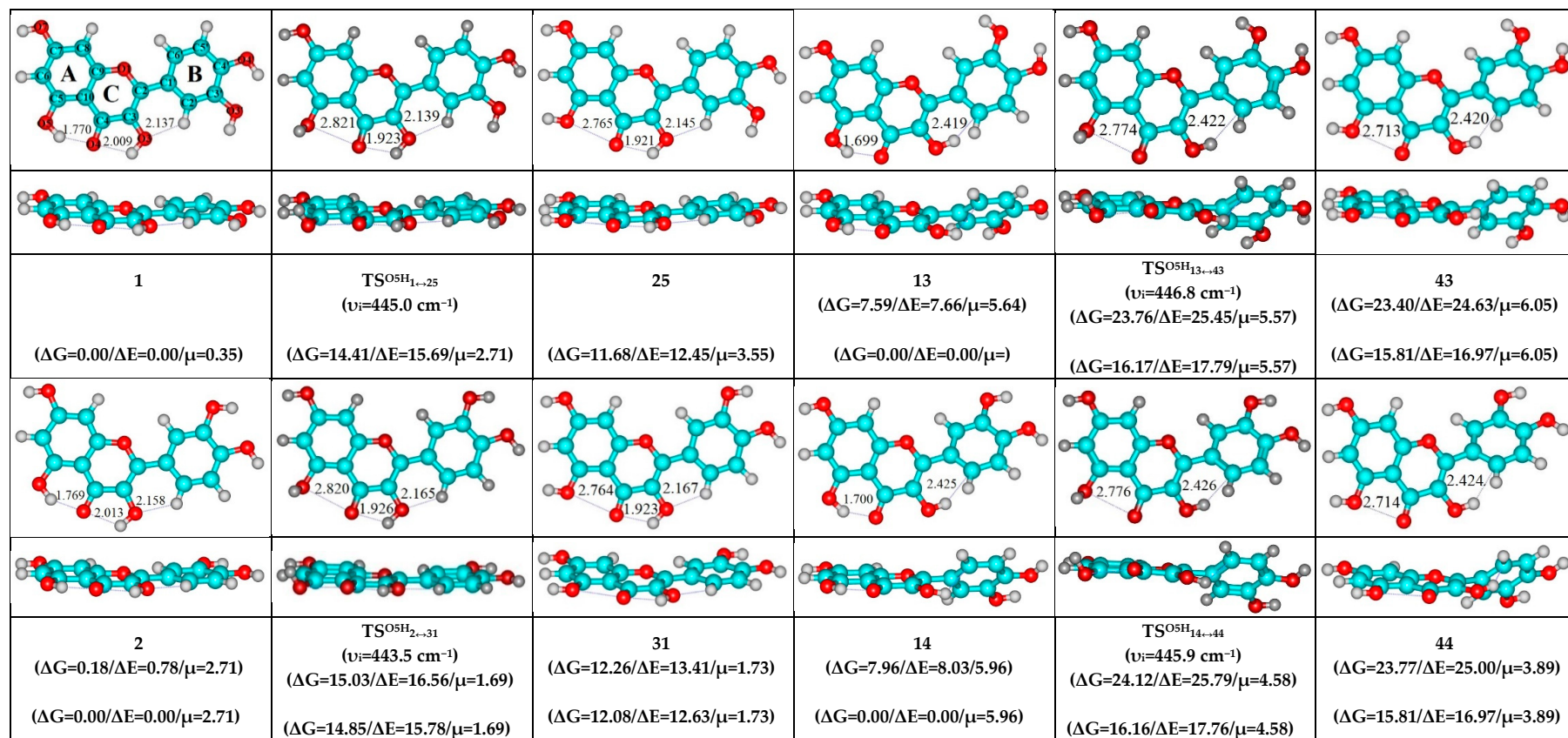


Figure 2. Cont.

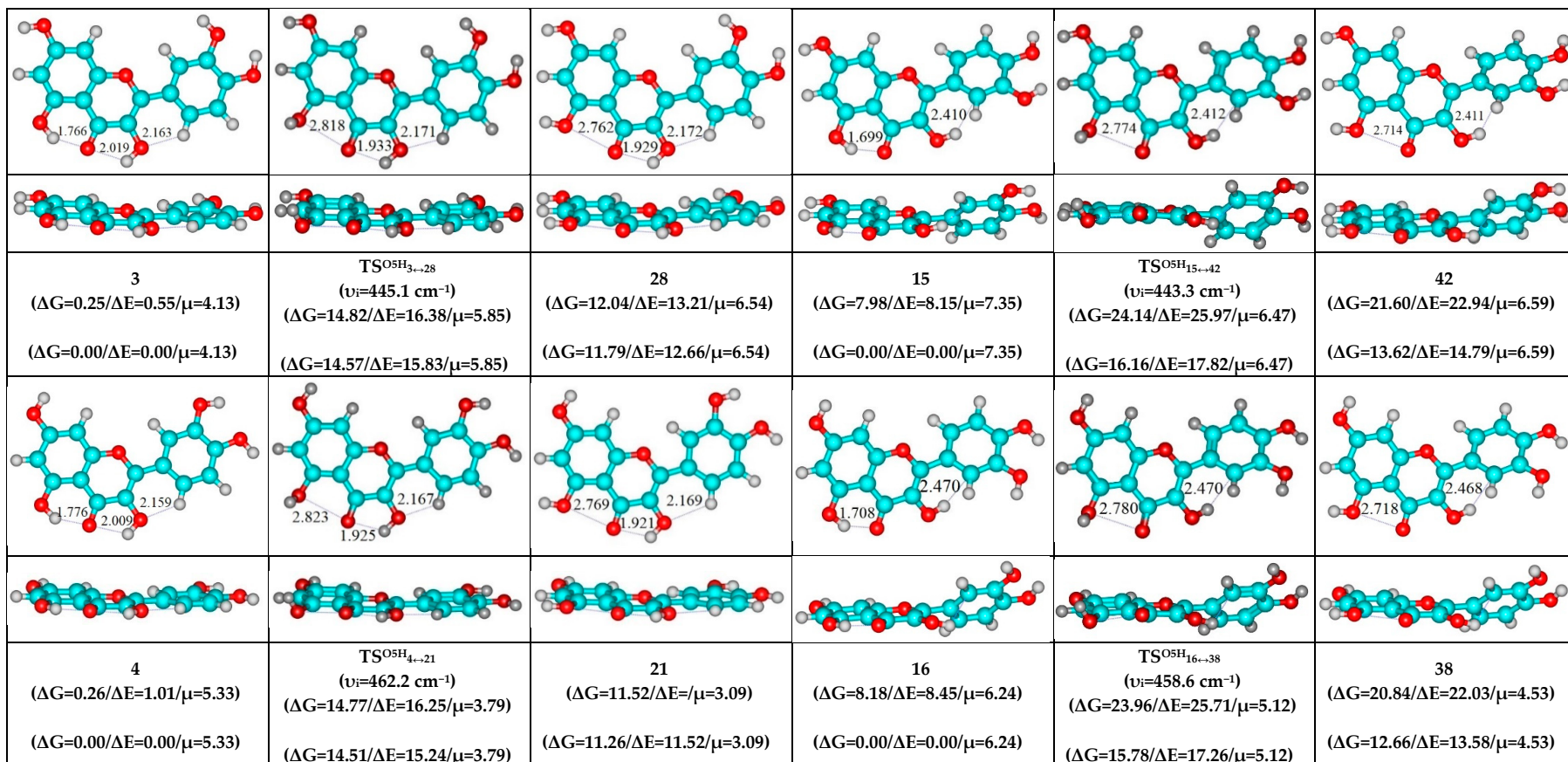


Figure 2. Cont.

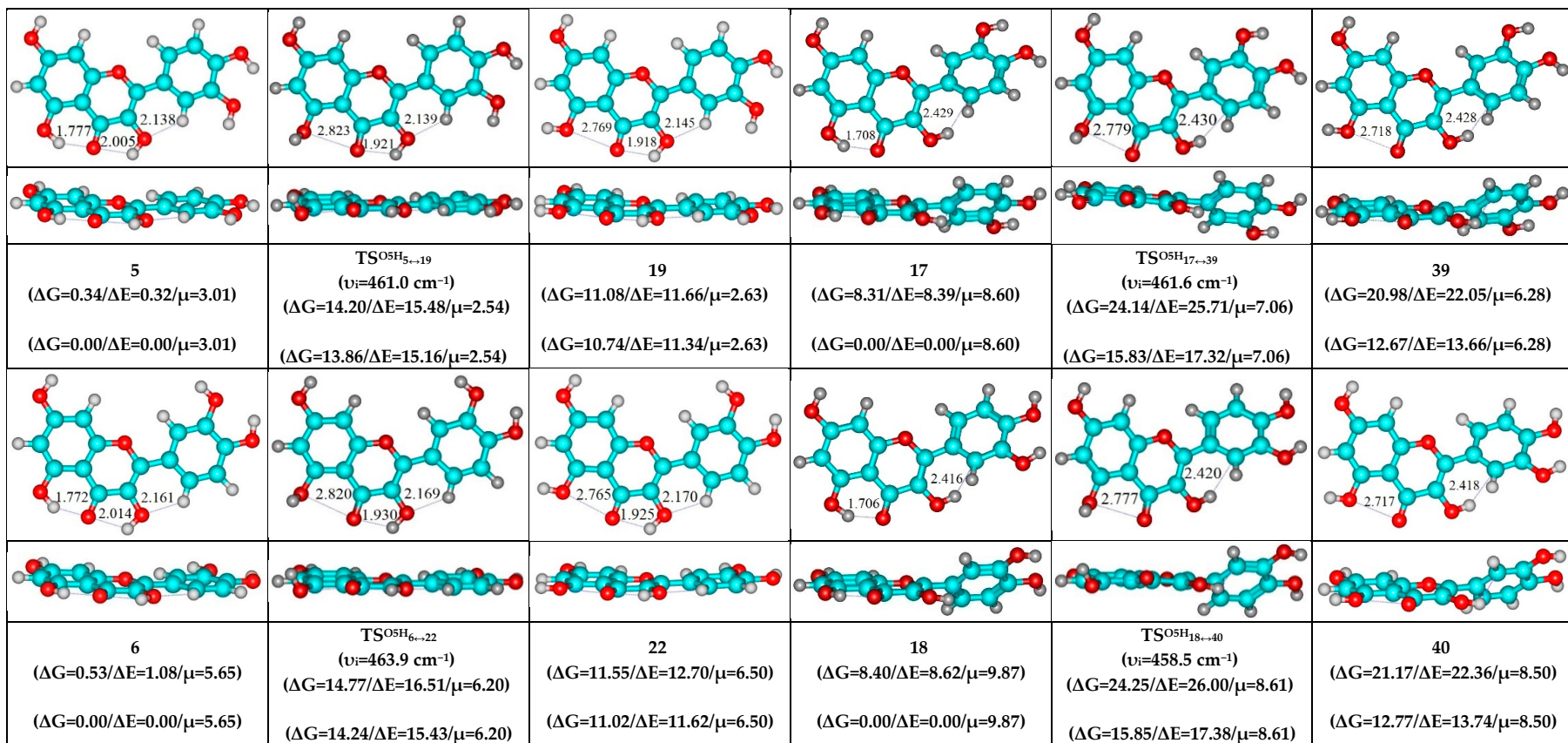


Figure 2. Cont.

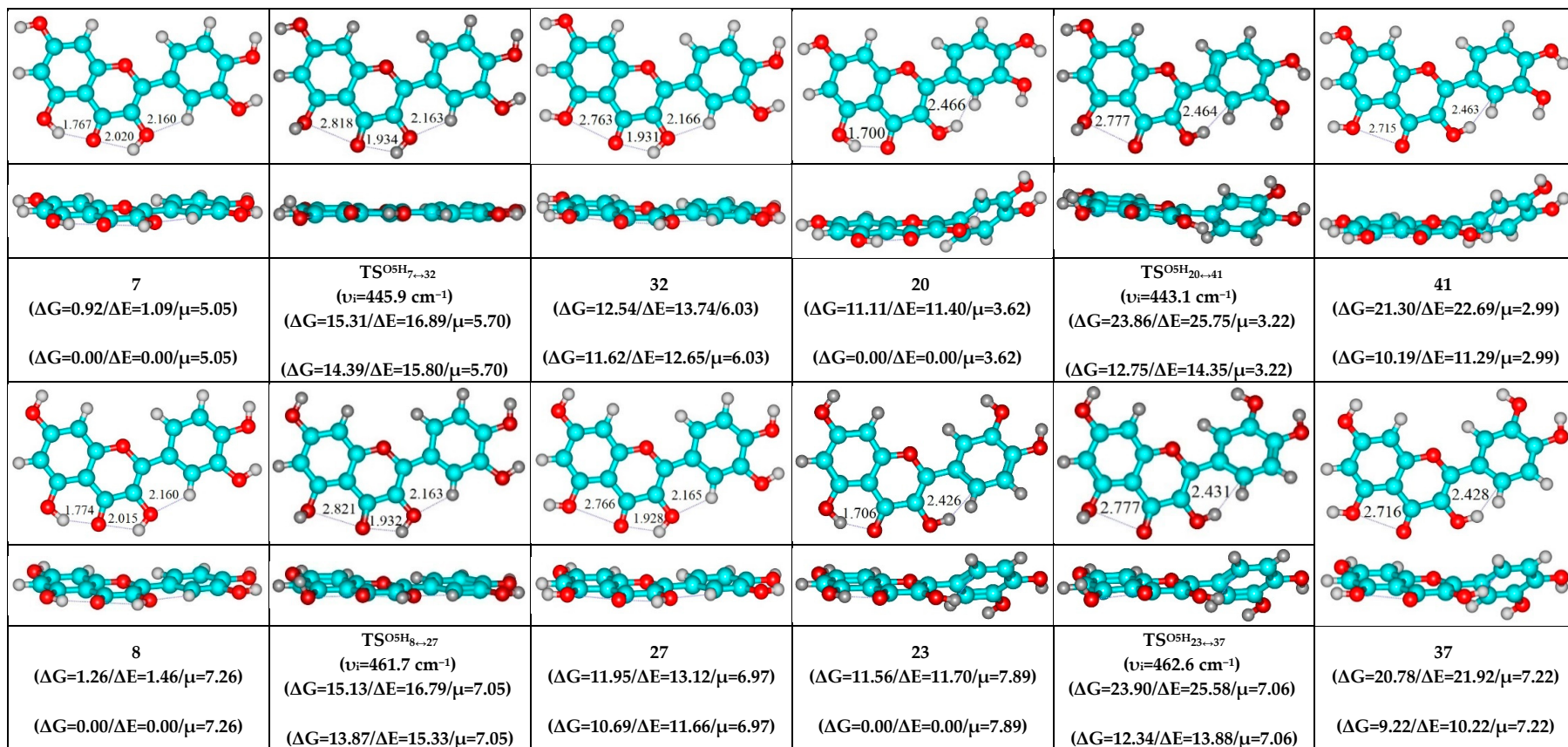


Figure 2. Cont.

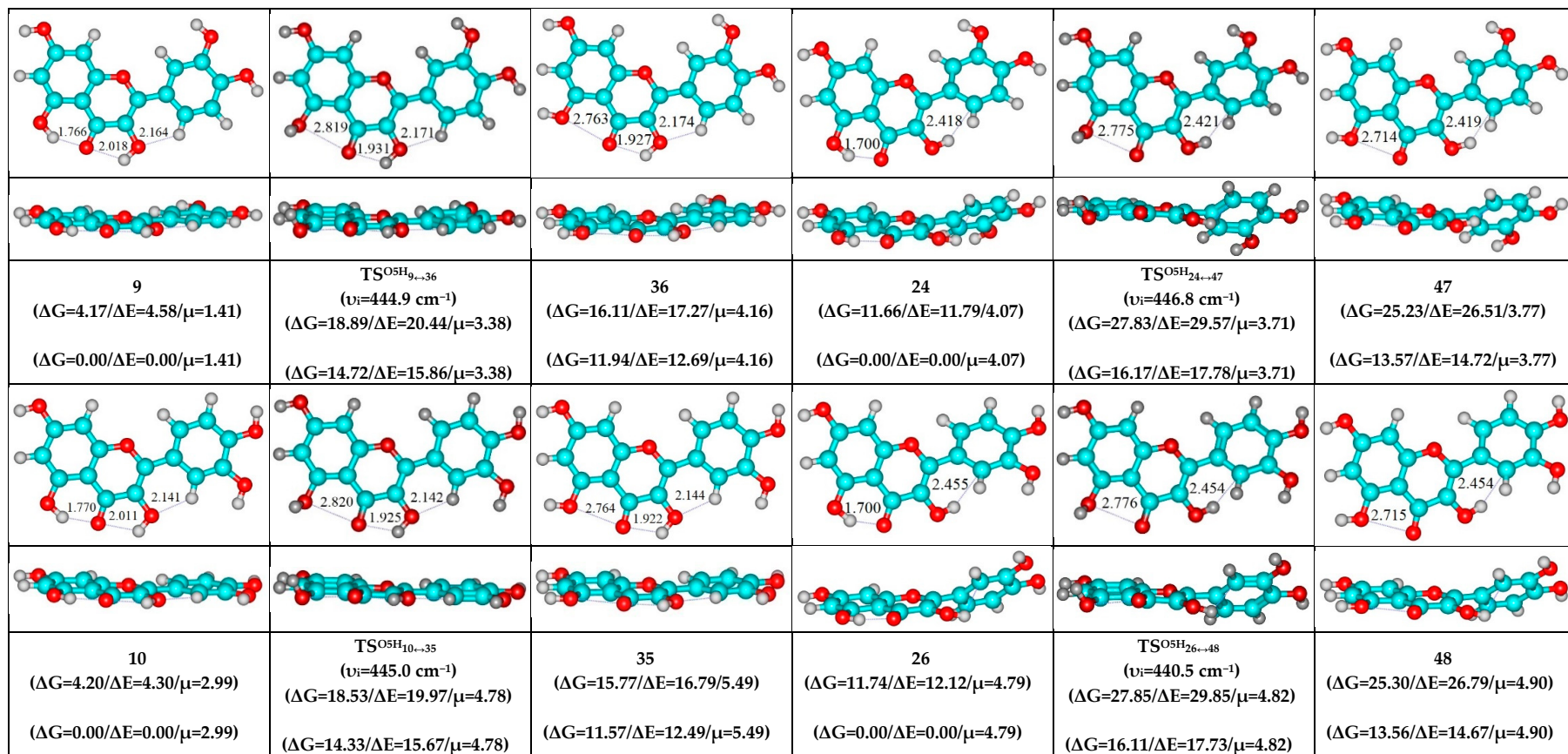


Figure 2. Cont.

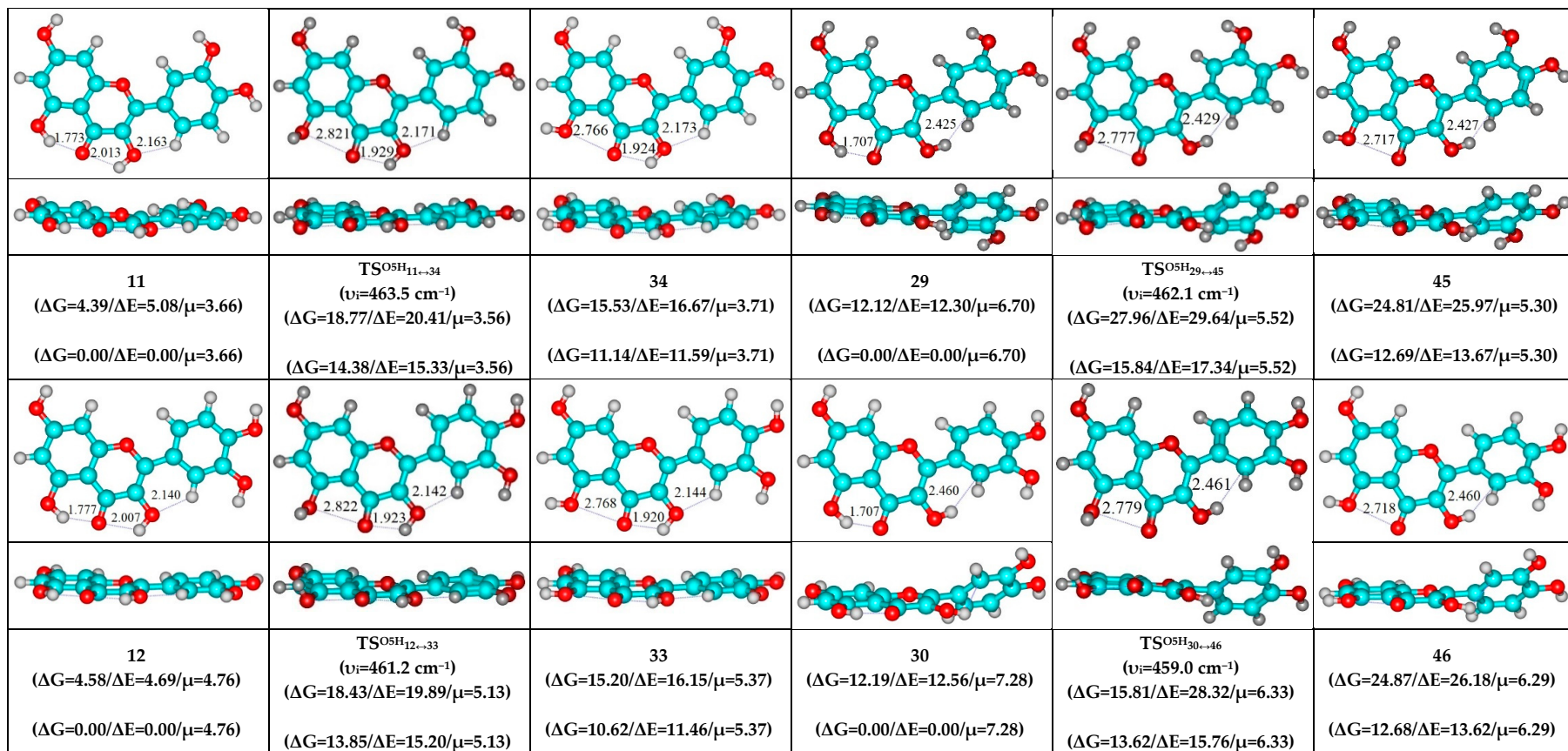


Figure 2. Geometrical structures of the quercetin molecule conformers and TSs with a non-perpendicularly oriented hydroxyl groups of their mutual interconversions via the mirror-symmetrical rotation of the O5H hydroxyl groups around the C5–O5 bonds, obtained at the MP2/6-311++G(2df,pd)//B3LYP/6-311++G(d,p) level of QM theory under standard conditions.

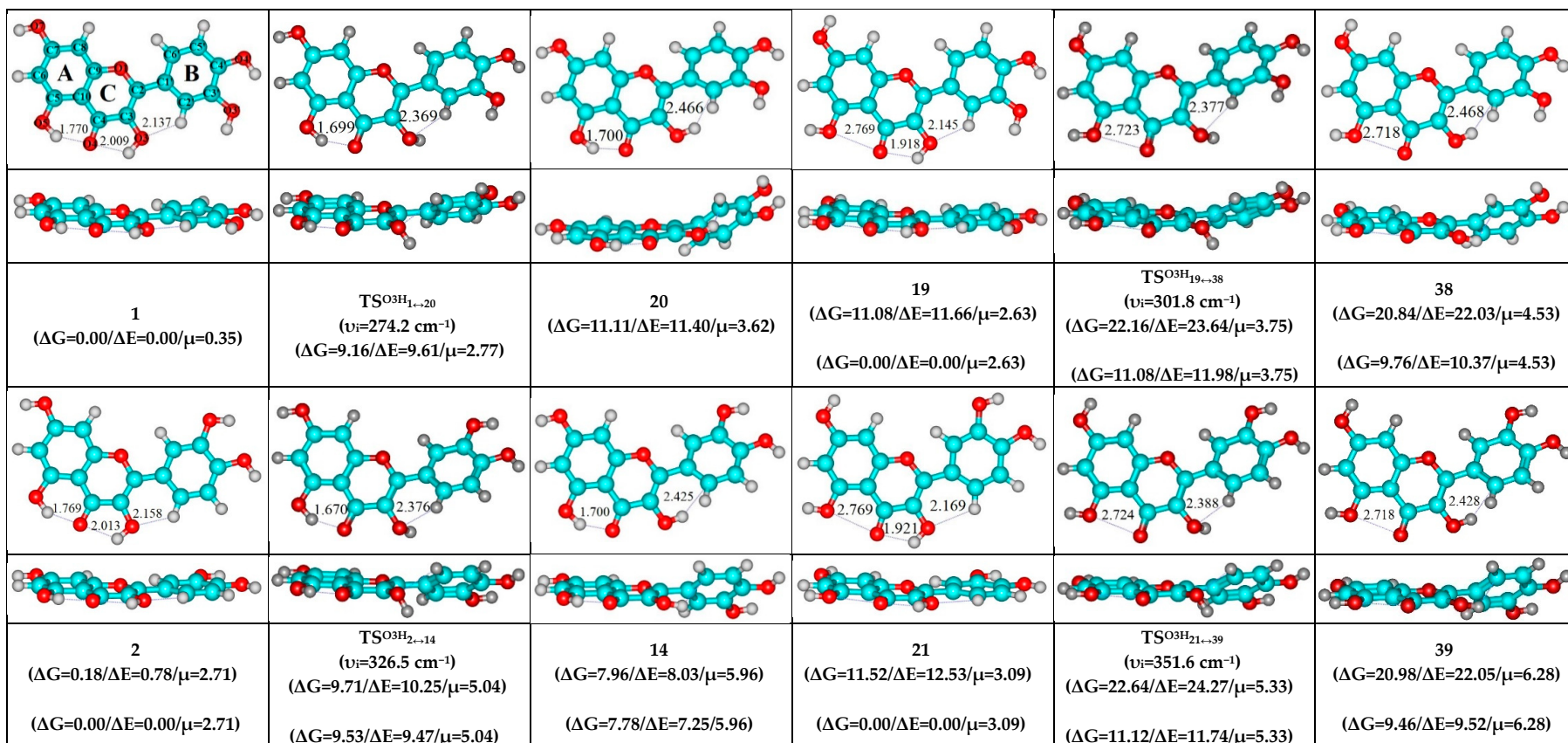


Figure 3. Cont.

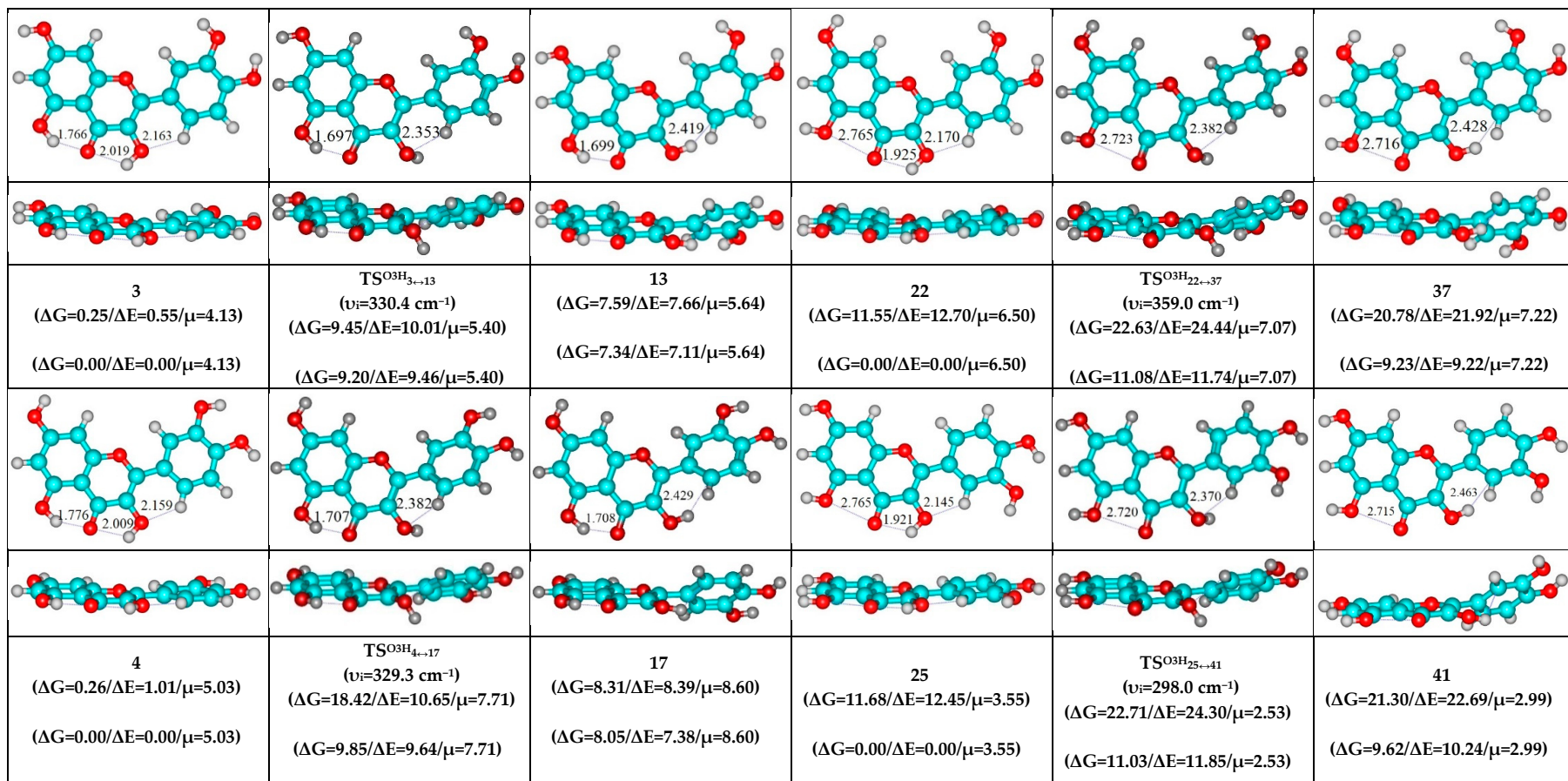


Figure 3. Cont.

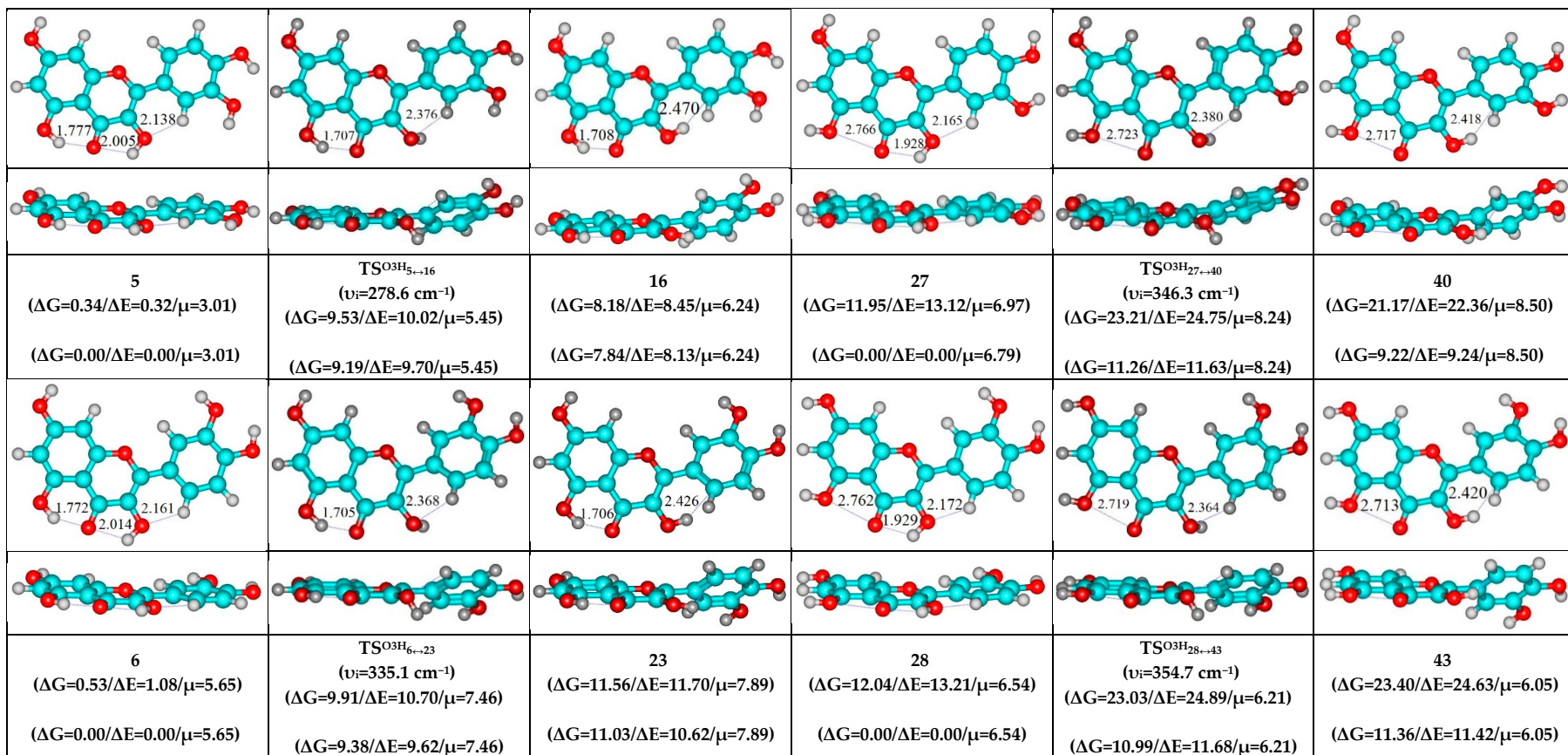


Figure 3. Cont.

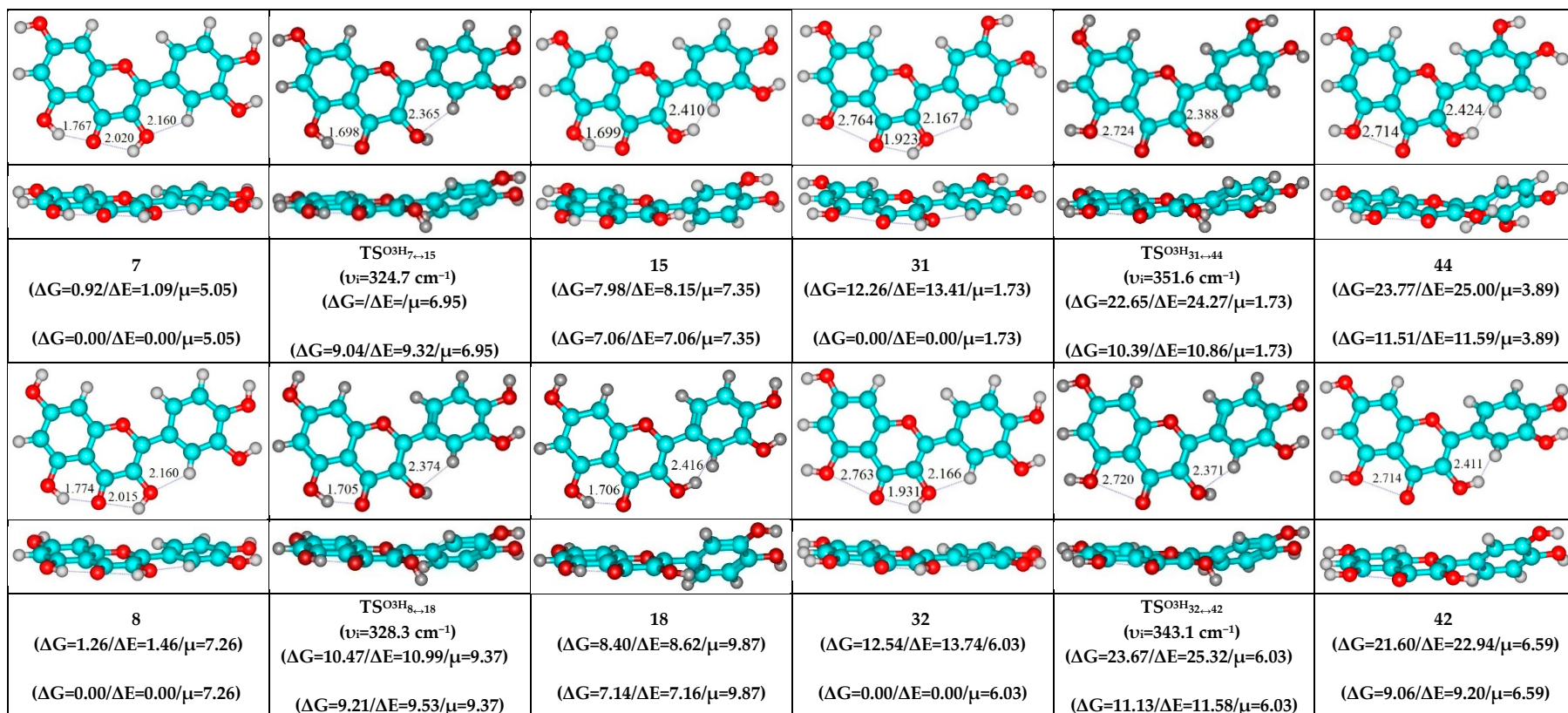


Figure 3. Cont.

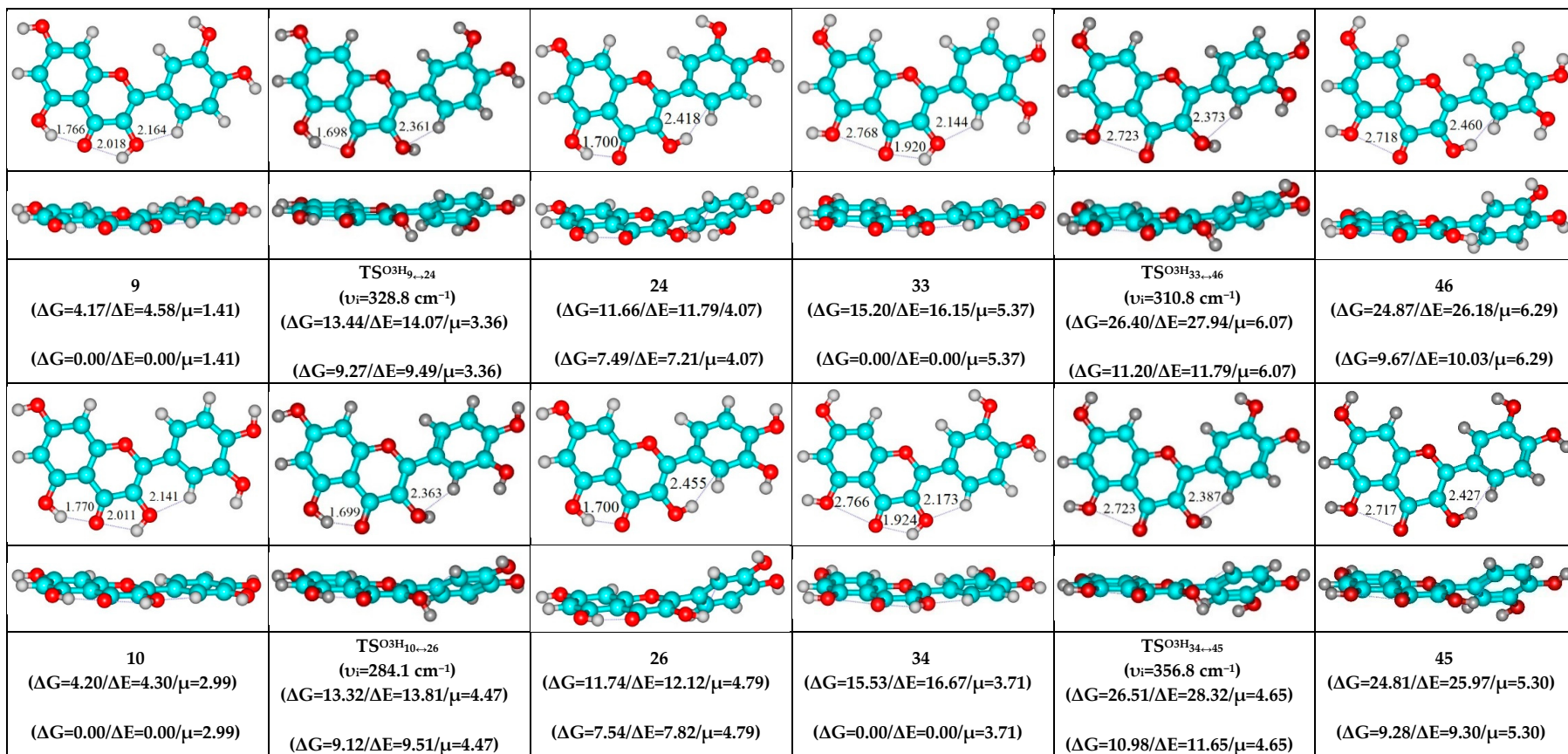


Figure 3. Cont.

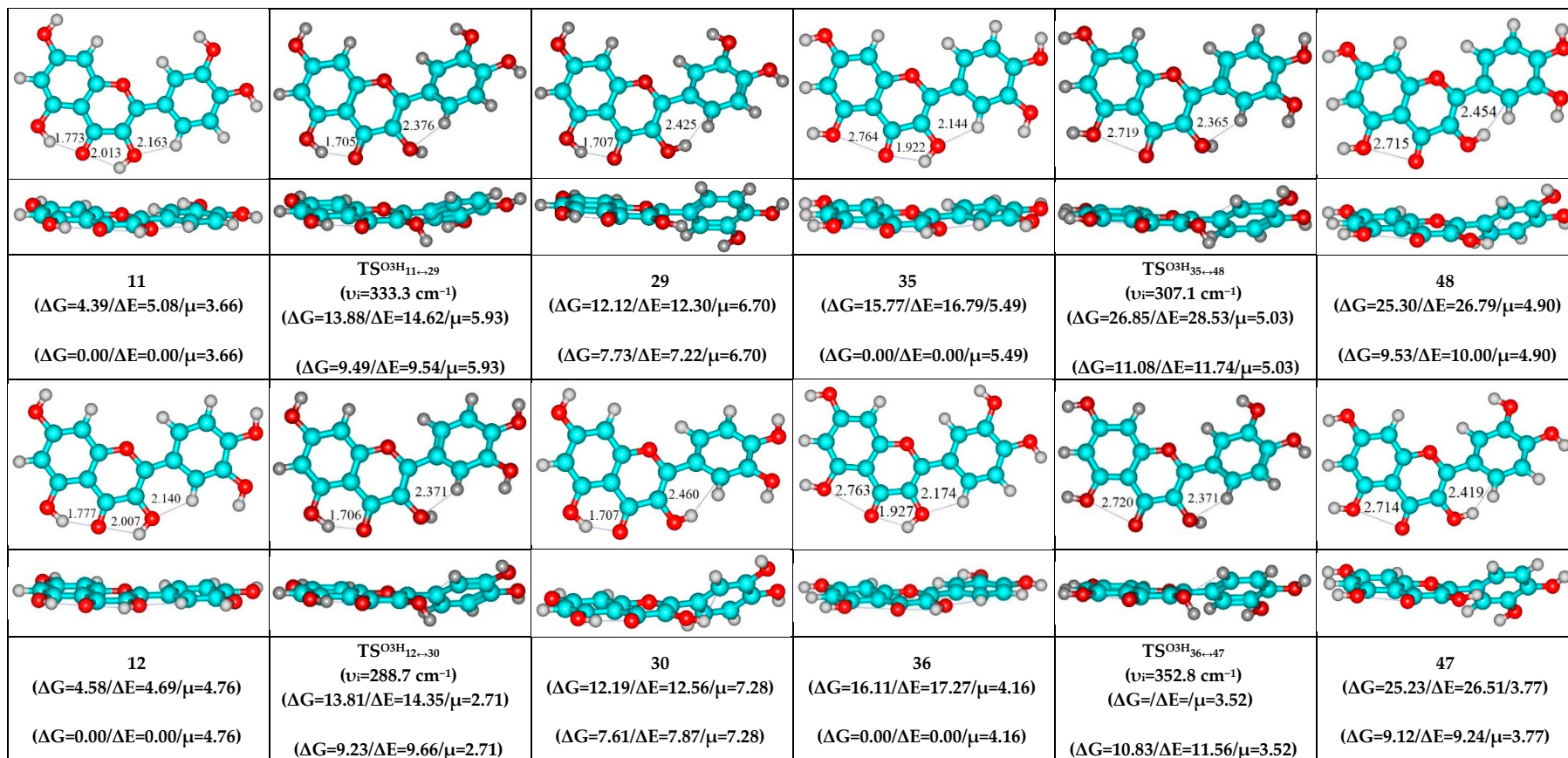


Figure 3. Geometrical structures of the quercetin molecule conformers and TSs with a non-perpendicularly oriented hydroxyl groups of their mutual interconversions via the mirror-symmetrical rotation of the O3H hydroxyl groups around the C3–O3 bonds, obtained at the MP2/6-311++G(2df,pd)//B3LYP/6-311++G(d,p) level of QM theory under standard conditions.

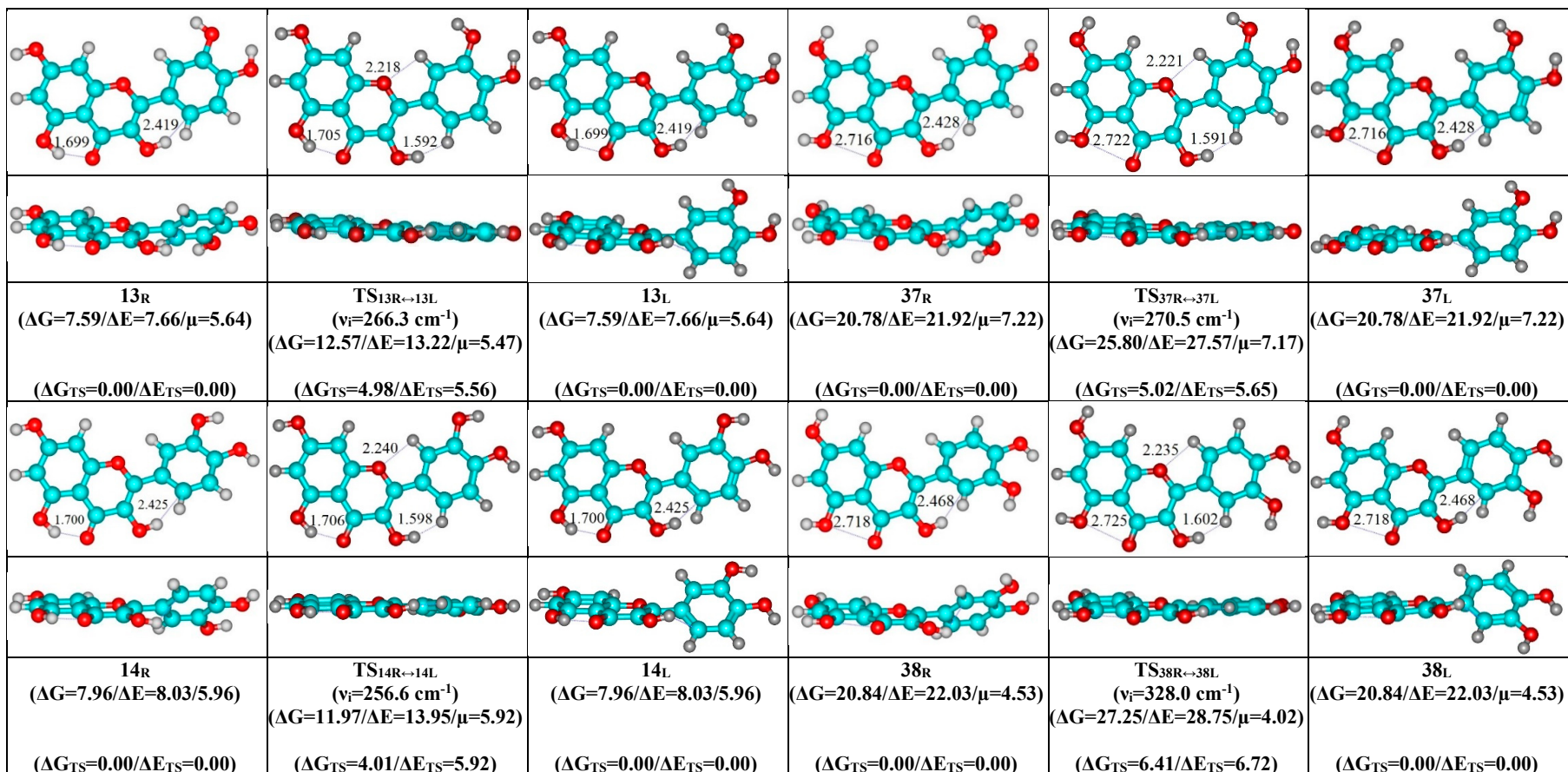


Figure 4. Cont.

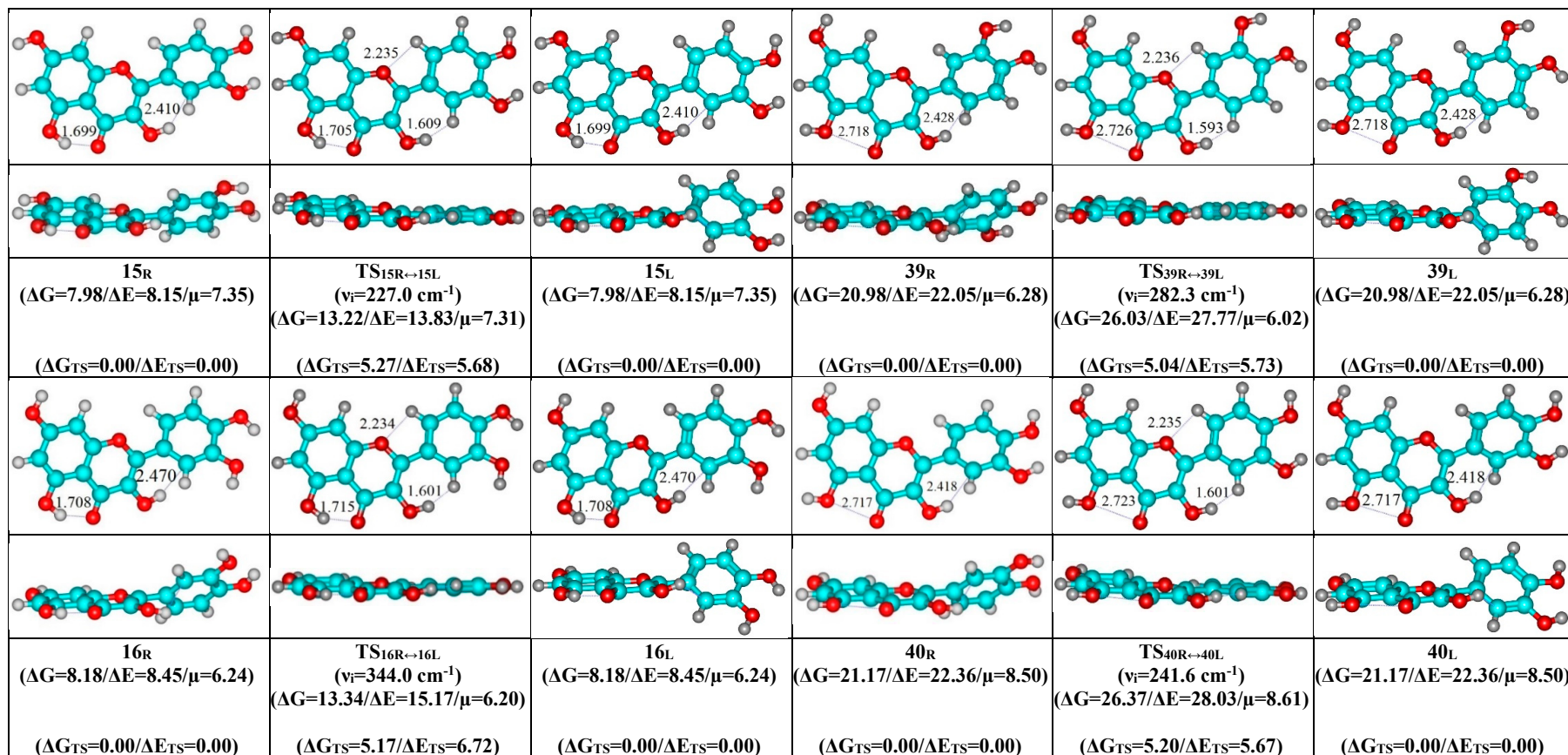


Figure 4. Cont.

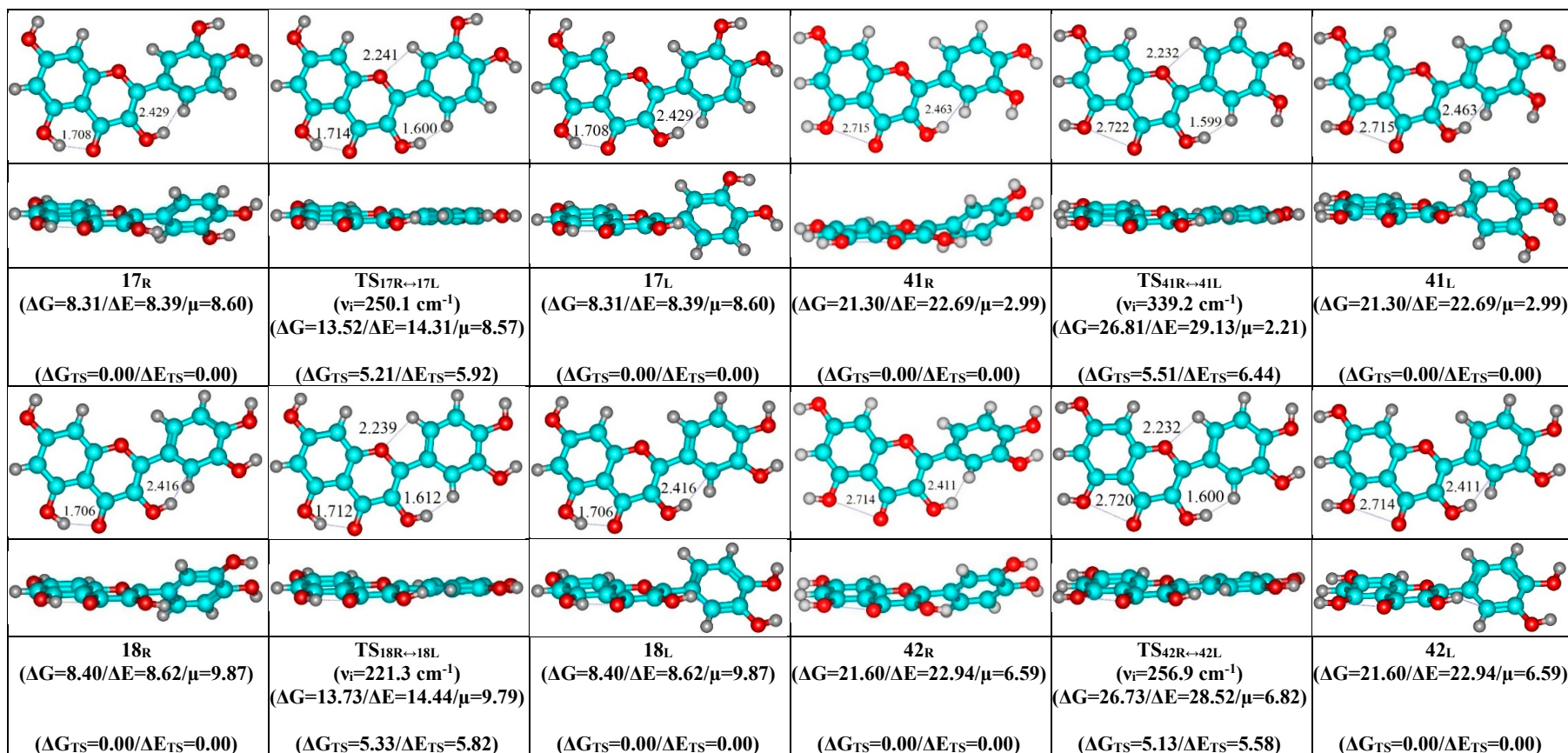


Figure 4. Cont.

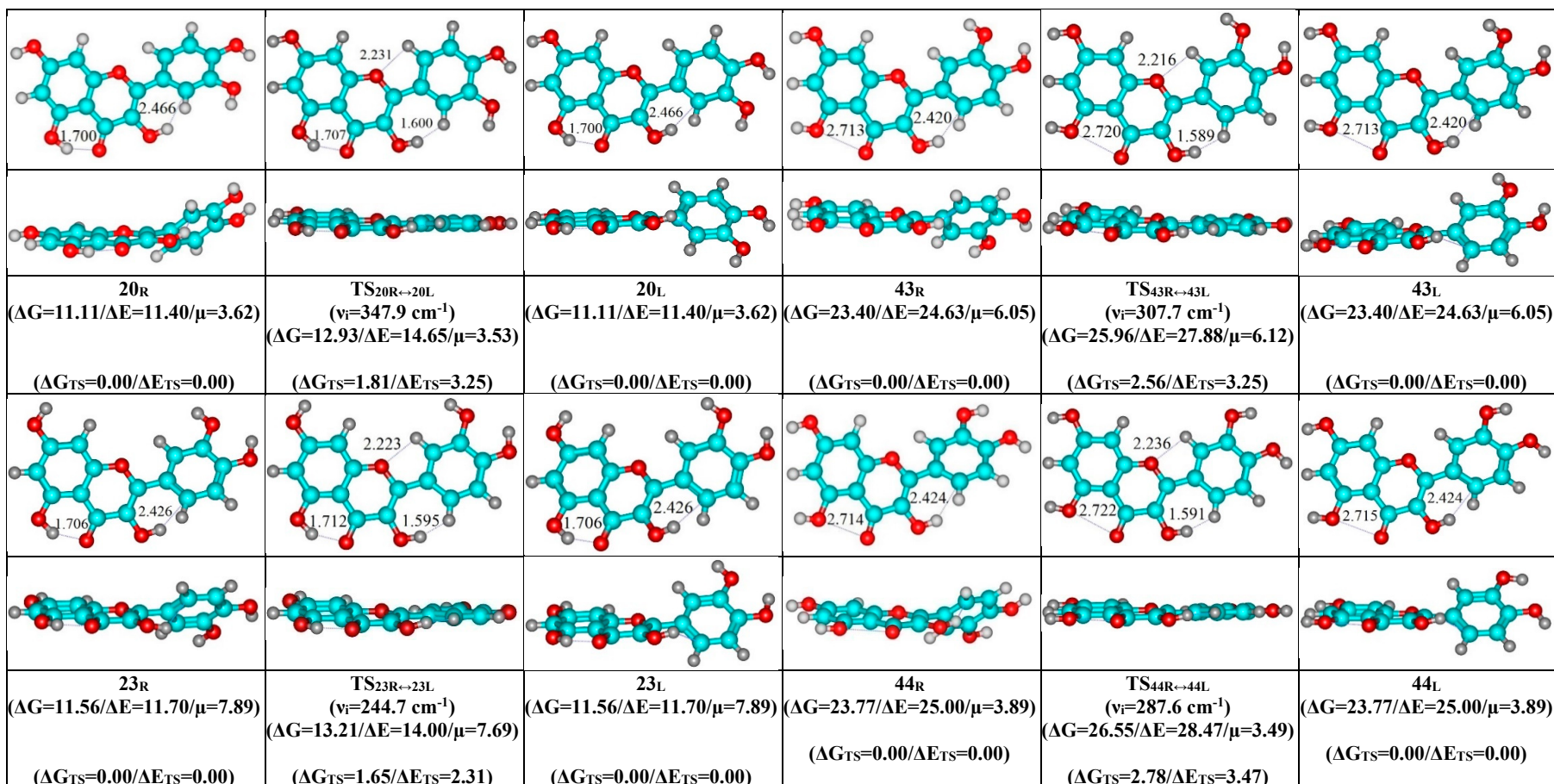


Figure 4. Cont.

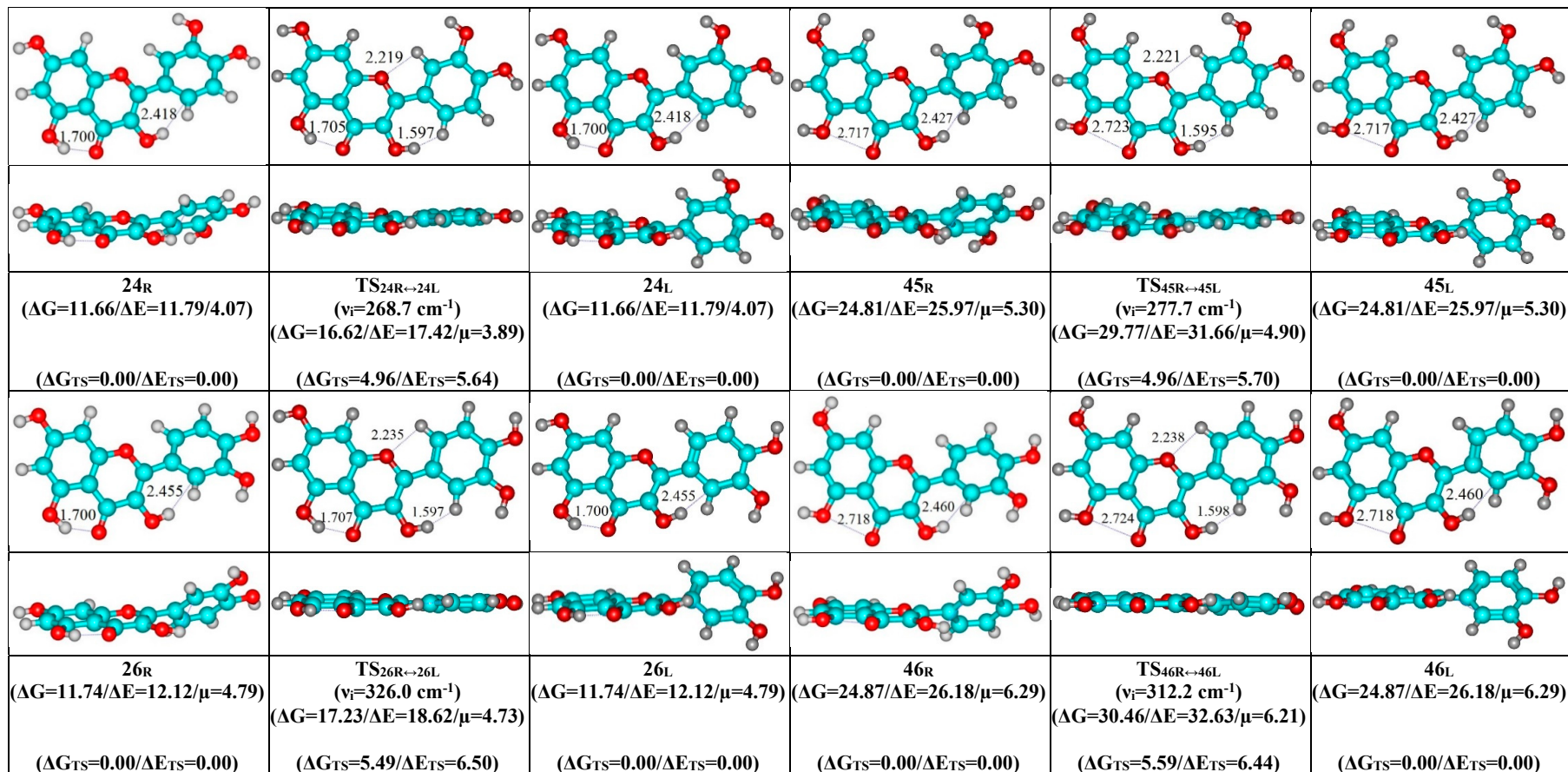


Figure 4. Cont.

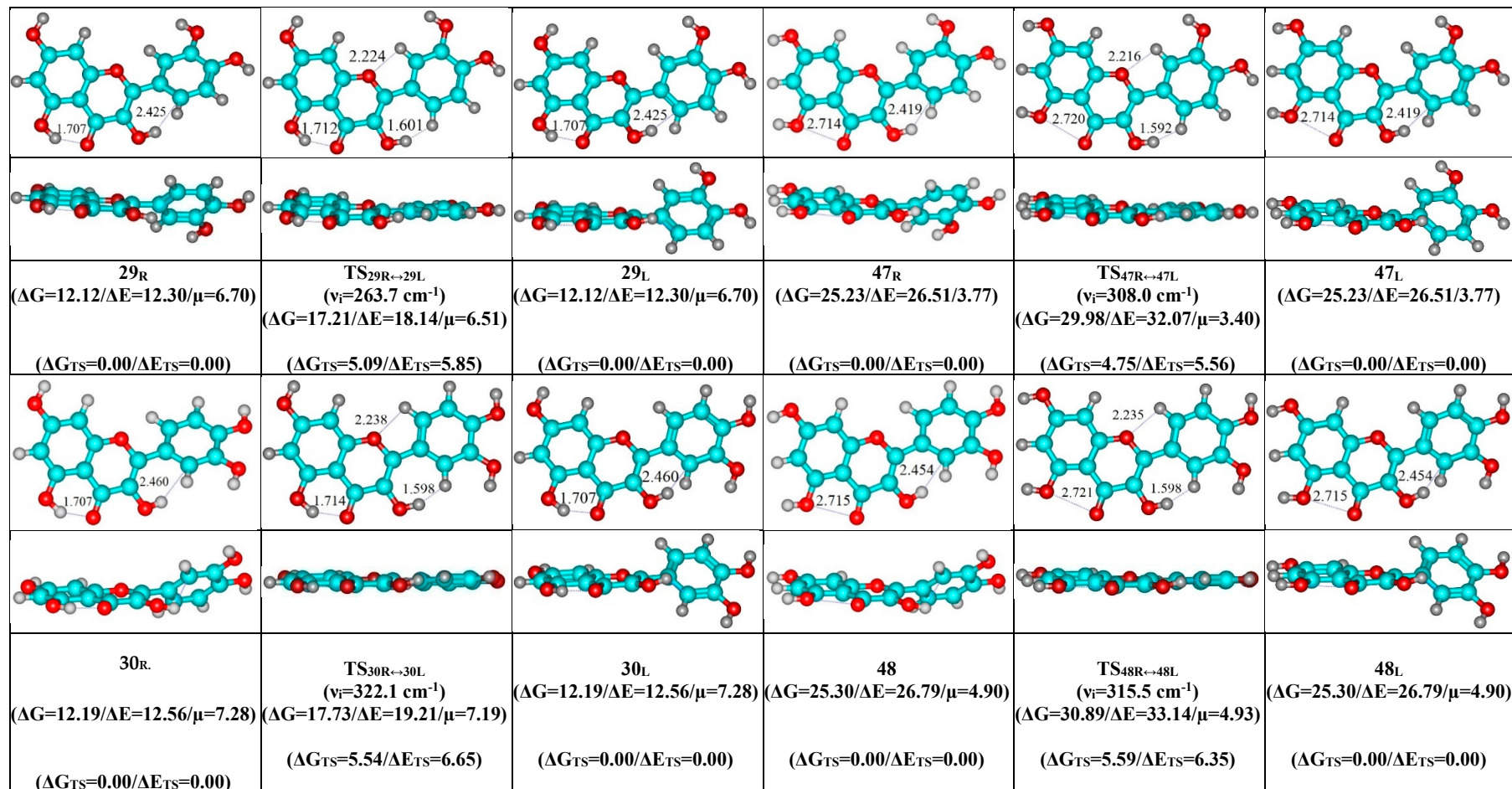


Figure 4. Geometrical structures of the non-planar conformers of the quercetin molecule and quasi-planar TSs of the interconversion of their enantiomers.

4. Conclusions

As a result of the *in silico* scrupulous investigation at the MP2/6-311++G(2df,pd)//B3LYP/6-311++G(d,p) level of QM theory, we investigated in details revealed conformational pathways, which are connected with the torsional mobility of the hydroxyl groups at the 3, 5 and 7 positions and interconversion of the enantiomers of the non-planar conformers of the quercetin molecule, and also their structural, energetic and polar physico-chemical characteristics, representing the hidden side of the conformational mobility of the quercetin molecule mentioned in the article title.

1. It was established, that conformational mobility of the isolated quercetin molecule, which is connected with the mirror-symmetric torsional mobility of its O₃H, O₅H and O₇H hydroxyl groups, were controlled by the 72 transitions states with the non-orthogonal geometry (C_1 point symmetry). In the cases of the turnings of the O₇H and O₅H hydroxyl groups, TSs were stabilized by the participation of the specific intramolecular interactions—attractive O₄ ... O₅ vdW contacts and C_{2'}/C_{6'}H...O₃ H-bonds, respectively. Activation barriers of the Gibbs free energies formed the following series under the standard conditions: $\Delta\Delta G_{TS}^{O7H}$ (3.51–4.24) < $\Delta\Delta G_{TS}^{O3H}$ (9.04–11.26) < $\Delta\Delta G_{TS}^{O5H}$ (12.34–16.17 kcal·mol⁻¹).
2. Conformational rearrangement of the O₃H and O₅H groups was partially controlled by the intramolecular specific interactions O₃H ... O₄, C_{2'}/C_{6'}H ... O₃, O₃H ... C_{2'}/C_{6'}, O₅H ... O₄ H-bonds and attractive O₄ ... O₅ vdW contacts, which were flexible and cooperative.
3. Mutual transformation of the enantiomers of the non-planar conformers of the quercetin molecule realized via the 24 quasi-planar TSs with C_1 point symmetry ($\Delta\Delta G_{TS} = 1.65$ –5.59 kcal·mol⁻¹), which were supported by the participation of the intramolecular O₃H...HC_{2'}/C_{6'} (4.7/4.8) and C_{2'}/C_{6'}H ... O₁ (4.7 kcal mol⁻¹) H-bonds.
4. All investigated conformational transitions were accompanied by the significant changes of the dipole moment of the molecule as by the absolute value, so by the spatial orientation.
5. Investigated conformational transformations were quite quick processes—time, which is necessary to acquire thermal equilibrium, did not exceed 6.5 ns.

Author Contributions: All authors participated in the statement of the task and idea of the investigation, preparation and discussion of the received results, preparation of the draft of the article and proofreading of the final version. All authors have read and agreed to the published version of the manuscript.

Funding: This research received no external funding. The APC was funded by MDPI.

Conflicts of Interest: The authors declare no conflict of interest.

References

1. Grytsenko, O.M.; Degtyarev, L.S.; Pilipchuk, L.B. Physico-chemical properties and electronic structure of quercetin. *Farmats. Zhurn.* **1992**, N2, 34–38.
2. Burda, S.; Oleszek, W. Antioxidant and antiradical activities of flavonoids. *J. Agric. Food Chem.* **2001**, *49*, 2774–2779. [[CrossRef](#)] [[PubMed](#)]
3. Grytsenko, O.M.; Pylypcchuk, L.B.; Bogdan, T.V.; Trygubenko, S.A.; Hovorun, D.M.; Maksutina, N.P. Keto-enol prototropic tautomerism of quercetin molecule: Quantum-chemical calculations. *Farmats. Zhurn.* **2003**, N5, 62–65.
4. Olejniczak, S.; Potrzebowski, M.J. Solid state NMR studies and density functional theory (DFT) calculations of conformers of quercetin. *Org. Biomol. Chem.* **2004**, *2*, 2315–2322. [[CrossRef](#)] [[PubMed](#)]
5. Bentz, A.B. A review of quercetin: Chemistry, antioxidant properties, and bioavailability. *J. Young Investig.* **2009**, *19*.
6. Nathiya, S.; Durga, M.; Devasena, T. Quercetin, encapsulated quercetin and its application—A review. *Int. J. Pharm. Pharm. Sci.* **2014**, *10*, 20–26.
7. David, A.V.A.; Arulmoli, R.; Parasuraman, S. Overviews of biological importance of quercetin: A bioactive flavonoid. *Pharmacogn. Rev.* **2016**, *10*, 84–89.

8. van Acker, S.A.; de Groot, M.J.; van den Berg, D.J.; Tromp, M.N.; Donné-Op den Kelder, G.; van der Vijgh, W.J.; Bast, A.A. A quantum chemical explanation of the antioxidant activity of flavonoids. *Chem. Res. Toxicol.* **1996**, *9*, 1305–1312. [[CrossRef](#)]
9. Bogdan, T.V.; Trygubenko, S.A.; Pylypczuk, L.B.; Potyayaylo, A.L.; Samijlenko, S.P.; Hovorun, D.M. Conformational analysis of the quercetin molecule. *Sci. Notes NaUKMA* **2001**, *19*, 456–460.
10. Trouillas, P.; Marsal, P.; Siri, D.; Lazzaroni, R.; Duroux, J.-C. A DFT study of the reactivity of OH groups in quercetin and taxifolin antioxidants: The specificity of the 3-OH site. *Food Chem.* **2006**, *97*, 679–688. [[CrossRef](#)]
11. Marković, Z.; Amić, D.; Milenković, D.; Dimitrić-Marković, J.M.; Marković, S. Examination of the chemical behavior of the quercetin radical cation towards some bases. *Phys. Chem. Chem. Phys.* **2013**, *15*, 7370–7378. [[CrossRef](#)] [[PubMed](#)]
12. Protsenko, I.O.; Hovorun, D.M. Conformational properties of quercetin: Quantum chemistry investigation. *Repts. Natl. Acad. Sci. Ukr.* **2014**, *N3*, 153–157. [[CrossRef](#)]
13. Vinnarasi, S.; Radhika, R.; Vijayakumar, S.; Shankar, R. Structural insights into the anti-cancer activity of quercetin on G-tetrad, mixed G-tetrad, and G-quadruplex DNA using quantum chemical and molecular dynamics simulations. *J. Biomol. Struct. Dyn.* **2019**. [[CrossRef](#)] [[PubMed](#)]
14. D’Andrea, G. Quercetin: A flavonol with multifaceted therapeutic applications? *Fitoterapia* **2015**, *106*, 256–271. [[CrossRef](#)]
15. Tu, B.; Liu, Z.-J.; Chen, Z.-F.; Ouyang, Y.; Hu, Y.-J. Understanding the structure–activity relationship between quercetin and naringenin: In vitro. *RSC Adv.* **2015**, *5*, 106171–106181. [[CrossRef](#)]
16. Brovarets’, O.O.; Hovorun, D.M. Conformational diversity of the quercetin molecule: A quantum-chemical view. *J. Biomol. Struct. Dyn.* **2019**. [[CrossRef](#)]
17. Brovarets’, O.O.; Hovorun, D.M. Conformational transitions of the quercetin molecule via the rotations of its rings: A comprehensive theoretical study. *J. Biomol. Struct. Dyn.* **2019**. [[CrossRef](#)]
18. Brovarets’, O.O.; Protsenko, I.O.; Hovorun, D.M. Computational design of the conformational and tautomeric variability of the quercetin molecule. In Proceedings of the 6th Young Medicinal Chemist Symposium (EFMC-YMCS 2019), Athens, Greece, 5–6 September 2019; p. 50.
19. Brovarets’, O.O.; Protsenko, I.O.; Hovorun, D.M. Comprehensive analysis of the potential energy surface of the quercetin molecule. In Proceedings of the Bioheterocycles 2019, XVIII International Conference on Heterocycles in Bioorganic Chemistry, Ghent, Belgium, 17–20 June 2019; p. 84.
20. Brovarets’, O.O.; Protsenko, I.O.; Zaychenko, G. Computational modeling of the tautomeric interconversions of the quercetin molecule. In Proceedings of the International Symposium “EFMC-ACSMEDI Medicinal Chemistry Frontiers 2019” (MedChemFrontiers 2019), Krakow, Poland, 10–13 June 2019; p. 114.
21. Jovanovic, S.V.; Steenken, S.; Hara, Y.; Simic, M.G. Reduction potentials of flavonoid and model phenoxyl radicals. Which ring in flavonoids is responsible for antioxidant activity? *J. Chem. Soc. Trans.* **1996**, *2*, 2497–2504. [[CrossRef](#)]
22. Rice-Evans, C.A.; Miller, N.J.; Paganga, G. Structure-antioxidant activity relationships of flavonoids and phenolic acids. *Free Radical Med.* **1996**, *20*, 933–956. [[CrossRef](#)]
23. Rasulev, B.F.; Abdullaev, N.D.; Syrov, V.N.; Leszczynski, J. A Quantitative Structure-Activity Relationship (QSAR) study of the antioxidant activity of flavonoids. *QSAR Comb. Sci.* **2005**, *24*, 1056–1065. [[CrossRef](#)]
24. Gao, S.; Sofic, E.; Prior, R.L. Antioxidant and prooxidant behavior of flavonoids: Structure-activity relationships. *Free Radic. Biol. Med.* **1997**, *22*, 749–760.
25. Domagała, S.; Munshi, P.; Ahmed, M.; Guillot, B.; Jelsch, C. Structural analysis and multipole modelling of quercetin monohydrate—A quantitative and comparative study. *Acta Cryst. Sect. B Struct. Sci.* **2010**, *67*, 63–78. [[CrossRef](#)] [[PubMed](#)]
26. Dhaouadi, Z.; Nsangou, M.; Garrab, N.; Anouar, E.H.; Marakchi, K.; Lahmar, S. DFT study of the reaction of quercetin with ·O₂ and ·OH radicals. *J. Mol. Struct. THEOCHEM* **2009**, *904*, 35–42. [[CrossRef](#)]
27. Yang, Y.; Zhao, J.; Li, Y. Theoretical study of the ESIPT process for a new natural product quercetin. *Sci. Repts.* **2016**, *6*, 32152. [[CrossRef](#)]
28. Eliel, E.; Wilen, S.H.; Mander, L.N. *Stereochemistry of Organic Compounds*; Wiley: New York, NY, USA, 1994.
29. Guijarro, A. *The Origin of Chirality in the Molecules of Life: A Revision from Awareness to the Current Theories and Perspectives of this Unsolved Problem*; Royal Society of Chemistry: Cambridge, UK, 2008.

30. Palafox, M.A. Molecular structure differences between the antiviral nucleoside analogue 5-iodo-2'-deoxyuridine and the natural nucleoside 2'-deoxythymidine using MP2 and DFT methods: Conformational analysis, crystal simulations, DNA pairs and possible behavior. *J. Biomol. Struct. Dyn.* **2014**, *32*, 831–851. [CrossRef]
31. Tirado-Rives, J.; Jorgensen, W.L. Performance of B3LYP Density Functional Methods for a large set of organic molecules. *J. Chem. Theory Comput.* **2008**, *4*, 297–306. [CrossRef]
32. Parr, R.G.; Yang, W. *Density-Functional Theory of Atoms and Molecules*; Oxford University Press: Oxford, UK, 1989.
33. Lee, C.; Yang, W.; Parr, R.G. Development of the Colle-Salvetti correlation-energy formula into a functional of the electron density. *Phys. Rev. B* **1988**, *37*, 785–789. [CrossRef]
34. Frisch, M.J.; Trucks, G.W.; Schlegel, H.B.; Scuseria, G.E.; Robb, M.A.; Cheeseman, J.R.; Scalmani, G.; Barone, V.; Petersson, G.A.; Nakatsuji, H.; et al. *GAUSSIAN 09*; Revision B.01; Gaussian Inc.: Wallingford, CT, USA, 2010.
35. Brovarets', O.O.; Hovorun, D.M. Atomistic understanding of the C-T mismatched DNA base pair tautomerization via the DPT: QM and QTAIM computational approaches. *J. Comput. Chem.* **2013**, *34*, 2577–2590. [CrossRef]
36. Brovarets', O.O.; Tsiupa, K.S.; Hovorun, D.M. Non-dissociative structural transitions of the Watson-Crick and reverse Watson-Crick A-T DNA base pairs into the Hoogsteen and reverse Hoogsteen forms. *Sci. Repts.* **2018**, *8*, 10371. [CrossRef]
37. Hratchian, H.P.; Schlegel, H.B. Finding minima, transition states, and following reaction pathways on ab initio potential energy surfaces. In *Theory and Applications of Computational Chemistry: The First 40 Years*; Dykstra, C.E., Frenking, G., Kim, K.S., Scuseria, G., Eds.; Elsevier: Amsterdam, The Netherlands, 2005; pp. 195–249.
38. Frisch, M.J.; Head-Gordon, M.; Pople, J.A. Semi-direct algorithms for the MP2 energy and gradient. *Chem. Phys. Lett.* **1990**, *166*, 281–289. [CrossRef]
39. Hariharan, P.C.; Pople, J.A. The influence of polarization functions on molecular orbital hydrogenation energies. *Theor. Chim. Acta* **1973**, *28*, 213–222. [CrossRef]
40. Krishnan, R.; Binkley, J.S.; Seeger, R.; Pople, J.A. Self-consistent molecular orbital methods. XX. A basis set for correlated wave functions. *J. Chem. Phys.* **1980**, *72*, 650–654. [CrossRef]
41. Atkins, P.W. *Physical Chemistry*; Oxford University Press: Oxford, UK, 1998.
42. Wigner, E. Über das Überschreiten von Potentialschwellen bei chemischen Reaktionen [Crossing of potential thresholds in chemical reactions]. *Zeits. Physik. Chem.* **1932**, *B19*, 203–216.
43. Keith, T.A. AIMAll (Version 10.07.01). 2010. Available online: aim.tkgristmill.com (accessed on 18 January 2020).
44. Matta, C.F.; Hernández-Trujillo, J. Bonding in polycyclic aromatic hydrocarbons in terms of the electron density and of electron delocalization. *J. Phys. Chem. A* **2003**, *107*, 7496–7504. [CrossRef]
45. Brovarets', O.O.; Yurenko, Y.P.; Hovorun, D.M. The significant role of the intermolecular CH···O/N hydrogen bonds in governing the biologically important pairs of the DNA and RNA modified bases: A comprehensive theoretical investigation. *J. Biomol. Struct. Dyn.* **2015**, *33*, 1624–1652. [CrossRef]
46. Lecomte, C.; Espinosa, E.; Matta, C.F. On atom–atom ‘short contact’ bonding interactions in crystals. *IUCrJ* **2015**, *2*, 161–163. [CrossRef]
47. Matta, C.F.; Castillo, N.; Boyd, R.J. Extended weak bonding interactions in DNA: π-stacking (base-base), base-backbone, and backbone-backbone interactions. *J. Phys. Chem. B* **2006**, *110*, 563–578. [CrossRef]
48. Nikolaienko, T.Y.; Bulavin, L.A.; Hovorun, D.M. Bridging QTAIM with vibrational spectroscopy: The energy of intramolecular hydrogen bonds in DNA-related biomolecules. *Phys. Chem. Chem. Phys.* **2012**, *14*, 7441–7447. [CrossRef]
49. Raczyńska, E.; Kosińska, W.; Ośmiałowski, B.; Gawinecki, R. Tautomeric equilibria in relation to π-electron delocalization. *Chem. Rev.* **2005**, *105*, 3561–3612. [CrossRef]
50. Brovarets', O.O.; Hovorun, D.M. A new era in the prototropic tautomerism of the quercetin molecule: A QM/QTAIM computational advances. *J. Biomol. Struct. Dyn.* **2019**. [CrossRef]



© 2020 by the authors. Licensee MDPI, Basel, Switzerland. This article is an open access article distributed under the terms and conditions of the Creative Commons Attribution (CC BY) license (<http://creativecommons.org/licenses/by/4.0/>).